Design, Synthesis, and Characterization of New Iron Chelators with Anti-Proliferative Activity: Structure−Activity Relationships of Novel Thiohydrazone Analogues

Danuta S. Kalinowski,[†] Philip C. Sharpe,[‡] Paul V. Bernhardt,*[,‡] and Des R. Richardson*[,†]

Iron Metabolism and Chelation Program, Department of Pathology and Bosch Institute, University of Sydney, Sydney, New South Wales 2006, Australia, and Centre for Metals in Biology, Department of Chemistry, University of Queensland, Brisbane, Queensland 4072, Australia

Received July 10, 2007

Di-2-pyridylketone isonicotinoyl hydrazone Fe chelators utilize the *N*,*N*,*O*-donor set and have moderate anti-proliferative effects. Their closely related *N*,*N*,*S*-thiosemicarbazone analogues, namely, the di-2-pyridylketone thiosemicarbazones, exhibit markedly increased anti-proliferative and redox activity, and this was thought to be due to the inclusion of a sulfur donor atom (Richardson, D. R. et al. *J. Med. Chem.* ***2006****, 49,* 6510−6521). To further examine the effect of donor atom identity on anti-proliferative activity, we synthesized thiohydrazone analogues of extensively examined aroylhydrazone chelators. The *O*,*N*,*S*-thiohydrazones exhibited decreased anti-proliferative effects compared to their parent aroylhydrazones and reduced redox activity. In contrast, the *N*,*N*,*S*-thiohydrazones showed vastly increased anti-proliferative activity compared to their hydrazone analogues, being comparable to potent thiosemicarbazones. Additionally, *N*,*N*,*S*-thiohydrazone complexes had reversible $Fe^{III/II}$ couples and exhibited increased redox activity. These observations demonstrate that the *N*,*N*,*S*-donor set is critical for potent anti-proliferative efficacy.

Introduction

The design and synthesis of iron (Fe) chelators has typically centered around their use for the treatment of Fe-overload disease.[1−3] However, the generation of appropriate chelators that sequester Fe from cancer cells represents a novel approach to chemotherapy.[4,5] Cancer cells show an increased requirement for Fe in comparison to their normal counterparts because of their rapid replication and thus demonstrate sensitivity to Fe-depletion.[5−9] This enhanced need of tumor cells for Fe is illustrated by their increased levels of transferrin receptor 1 that mediate a high rate of Fe uptake from the serum Fe transport protein, transferrin (Tf[a]).[7−9] By reducing intracellular Fe levels, various critical cellular processes dependent on Fe are disrupted. For instance, the enzyme involved in the rate-limiting step of DNA synthesis, ribonucleotide reductase (RR), contains Fe bound in the R2 subunit, which is critical for enzyme activity.[10−13] Thus, Fe-deprivation leads to loss of RR activity, and through this mechanism, chelators inhibit tumor growth. However, RR is not the only target of these ligands, with the expression of a number of molecules involved in cell cycle progression and metastasis and growth suppression being regulated by intracellular Fe levels.[14−19]

A number of chelators with potent anti-proliferative activity have been identified, with Tachpyridine,[20,21] 3-aminopyridine-2-carboxaldehyde thiosemicarbazone (3-AP, Figure 1A),[22−24] O-Trensox,[25] and some chelators of the pyridoxal isonicotinoyl hydrazone (H_2PIH) class[26−28] and their analogues[29,30] being appropriate for consideration.[5,31] Some of these chelators are also able to exert their cytotoxic effects through the redox cycling of their Fe complexes.[32−36] These complexes can interact with cellular oxidants and reductants allowing for interconversion between the Fe^{II} and Fe^{III} redox states.[6] This results in the production of cytotoxic reactive oxygen species (ROS), including the hydroxyl radical ($OH^{\bullet}$), which can initiate chemical reactions with many biomolecules.[6,37] For instance, oxidation of DNA and damage to mitochondria caused by ROS can lead to cell death.[37] Thus, some Fe chelators induce anti-tumor effects via two mechanisms, that is, Fe complexation and the production of ROS.[32,33]

The di-2-pyridylketone isonicotinoyl hydrazone (HPKIH) series of ligands (Figure 1A) that were previously developed within our laboratory demonstrated moderate anti-proliferative activity (IC_{50} = 1−42 μM) against the SK-N-MC neuroepithelioma cell line.[30] These ligands utilize an *N*,*N*,*O*-donor set.[38] The redox activity of the HPKIH series was demonstrated by their ability to enhance DNA plasmid degradation in the presence of H_2O_2 and stimulate benzoate hydroxylation in the presence of Fe^{II} and H_2O_2.[38,39] Furthermore, cyclic voltammetry of the Fe^{II}-PKIH complexes demonstrated that nucleophilic attack on the C═N-Fe group by the hydroxide anion occurred upon oxidation to the Fe^{III} state.[38] This irreversible electrochemistry resulted in the loss of the potentially high oxidizing ability of the Fe^{II}-PKIH complexes[38] and probably limited their anti-proliferative activity.

In the search for increasingly active chelators, the related di-2-pyridylketone thiosemicarbazone (HDpT; Figure 1A) analogues were synthesized and their biological activity evaluated.[32,33,40] These ligands, which utilize the *N*,*N*,*S*-donor set, demonstrated potent anti-proliferative activity *in vitro*[32,33,40] (IC_{50} = 0.01−5.20 μM) and *in vivo*.[32,40] This was thought to be mediated, at least in part, by their ability to promote redox cycling of Fe.[32,33] The dramatic increase in anti-neoplastic

* Corresponding author. Phone: +61-2-9036-6548. Fax: +61-2-9036-6549. E-mail: d.richardson@med.usyd.edu.au (D.R.R). Phone: +61-7-3365-4266. Fax: +61-7-3365-4299. E-mail: p.bernhardt@uq.edu.au (P.V.B.).
[†] University of Sydney.
[‡] University of Queensland.

[a] Abbreviations: 3-AP, 3-aminopyridine-2-carboxaldehyde thiosemicarbazone; DFO, desferrioxamine; HBPBH, 2-benzoylpyridine benzoyl hydrazone; HBPTBH, 2-benzoylpyridine thiobenzoyl hydrazone; HDpT, di-2-pyridylketone thiosemicarbazone; HDp44mT, di-2-pyridylketone 4,4-dimethyl-3-thiosemicarbazone; H_2NBH, 2-hydroxy-1-naphthaldehyde benzoyl hydrazone; H_2NIH, 2-hydroxy-1-naphthaldehyde isonicotinoyl hydrazone; H_2NTBH, 2-hydroxy-1-naphthaldehyde thiobenzoyl hydrazone; H_2PBH, pyridoxal benzoyl hydrazone; H_2PIH, pyridoxal isonicotinoyl hydrazone; HPKBH, di-2-pyridylketone benzoyl hydrazone; HPKIH, di-2-pyridylketone isonicotinoyl hydrazone; HPKTBH, di-2-pyridylketone thiobenzoyl hydrazone; H_2PTBH, pyridoxal thiobenzoyl hydrazone; H_2SBH, salicylaldehyde benzoyl hydrazone; H_2STBH, salicylaldehyde thiobenzoyl hydrazone; IBE, iron-binding equivalent; ROS, reactive oxygen species; RR, ribonucleotide reductase; Tf, transferrin.

10.1021/jm070839q CCC: $37.00
Published on Web 10/27/2007

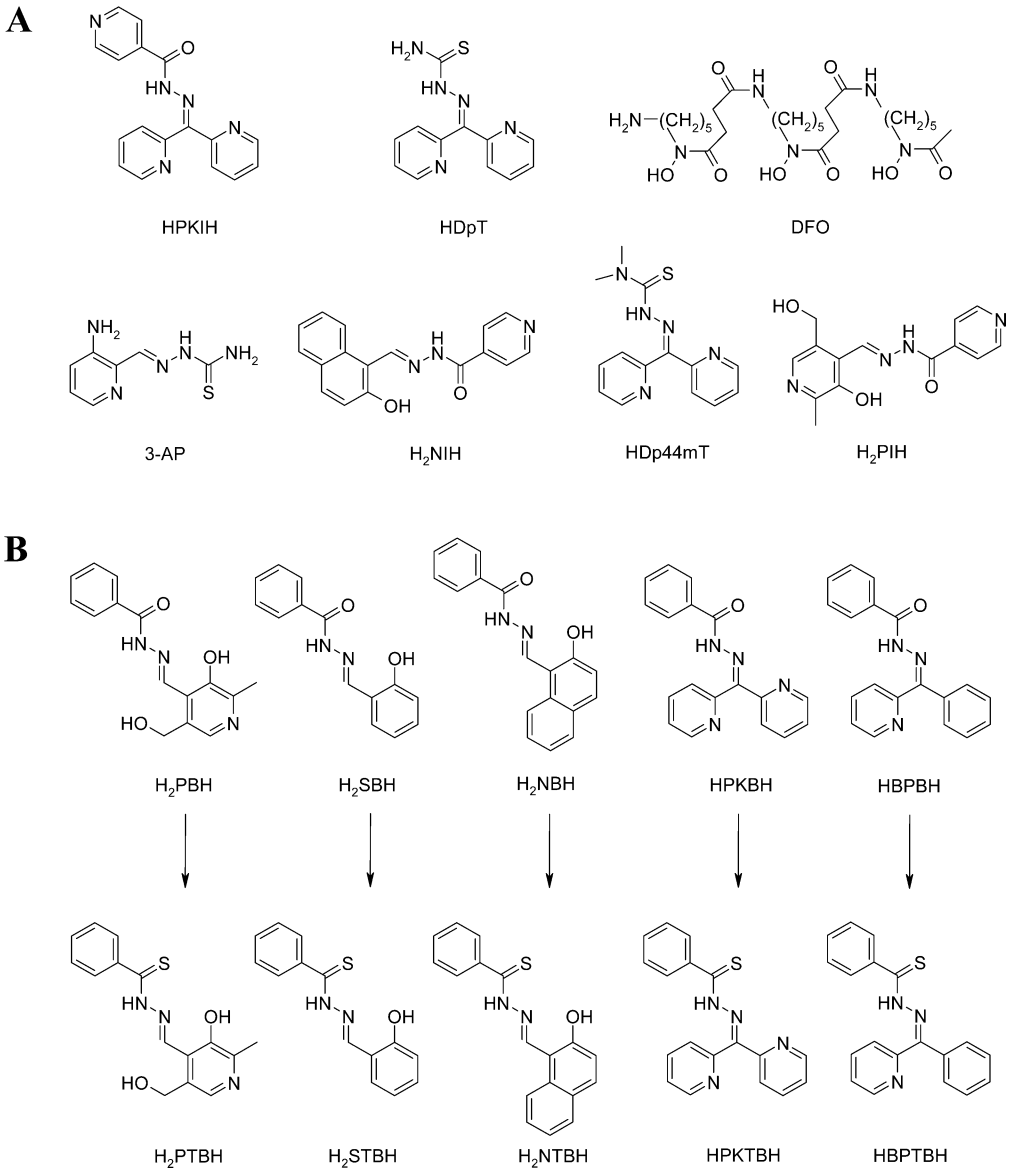

Figure 1. Chemical structures of iron chelators used in this study. (A) Di-2-pyridylketone isonicotinoyl hydrazone (HPKIH), di-2-pyridylketone thiosemicarbazone (HDpT), desferrioxamine (DFO), 3-aminopyridine-2-carboxaldehyde thiosemicarbazone (3-AP), 2-hydroxy-1-naphthaldehyde isonicotinoyl hydrazone (H_2NIH), di-2-pyridylketone 4,4-dimethyl-3-thiosemicarbazone (HDp44mT), and pyridoxal isonicotinoyl hydrazone (H_2PIH). (B) Comparison of the chemical structures of the parent oxygen analogues, pyridoxal benzoyl hydrazone (H_2PBH), salicylaldehyde benzoyl hydrazone (H_2SBH), 2-hydroxy-1-naphthaldehyde benzoyl hydrazone (H_2NBH), di-2-pyridylketone benzoyl hydrazone (HPKBH), and 2-benzoylpyridine benzoyl hydrazone (HBPBH) against their corresponding sulfur derivatives, pyridoxal thiobenzoyl hydrazone (H_2PTBH), salicylaldehyde thiobenzoyl hydrazone (H_2STBH), 2-hydroxy-1-naphthaldehyde thiobenzoyl hydrazone (H_2NTBH), di-2-pyridylketone thiobenzoyl hydrazone (HPKTBH), and 2-benzoylpyridine thiobenzoyl hydrazone (HBPTBH), respectively.

activity of these ligands was attributed to the replacement of the oxygen-containing hydrazide portion of the HPKIH analogues to the sulfur-containing thiosemicarbazide moiety of the HDpT series.[33] It was postulated that changing the donating oxygen atom to sulfur may be responsible for the increased redox activity and anti-tumor activity of the HDpT series.[33]

In an attempt to investigate the effect of donor atom identity on anti-tumor activity, in the current study, we designed and synthesized a novel range of thiohydrazone analogues, on the basis of the structure of previously evaluated oxygen-containing hydrazone chelators (Figure 1B). These hydrazones included pyridoxal benzoyl hydrazone (H_2PBH),[28,41,42] salicylaldehyde benzoyl hydrazone (H_2SBH),[41] 2-hydroxy-1-naphthaldehyde benzoyl hydrazone (H_2NBH),[41] di-2-pyridylketone benzoyl hydrazone (HPKBH),[30,38] and 2-benzoylpyridine benzoyl hydrazone (HBPBH; Figure 1B). The related thiohydrazone analogues included pyridoxal thiobenzoyl hydrazone (H_2PTBH), salicylaldehyde thiobenzoyl hydrazone (H_2STBH), 2-hydroxy-1-naphthaldehyde thiobenzoyl hydrazone (H_2NTBH), di-2-pyridylketone thiobenzoyl hydrazone (HPKTBH), and 2-benzoylpyridine thiobenzoyl hydrazone (HBPTBH; Figure 1B). The latter ligands incorporate the thiobenzoyl hydrazone moiety, replacing the carbonyl oxygen donor atom of their parent ligand with sulfur. Interestingly, we were able to identify several modified forms of these ligands, some of which exist in equilibrium with the thiohydrazone Schiff base form. The structure−activity relationships of these sulfur analogues is examined in comparison with their parent hydrazone analogues in terms of further designing more effective compounds for the treatment of cancer.

Results and Discussion

Synthesis and Characterization of Thiohydrazone Analogues. Replacement of the carbonyl oxygen with sulfur in the

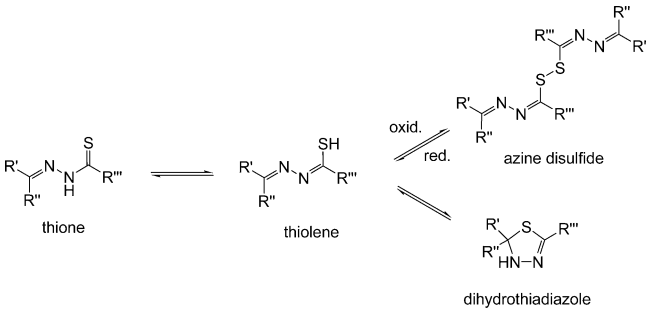

Figure 2. Schematic diagram illustrating the thione−thiolene tautomerism of thiohydrazones and the subsequent formation of their derivatives: an azine disulfide dimer and the dihydrothiadiazole.

ligands (Figure 1B) was an important synthetic strategy to investigate the structure−activity relationships of the aroylhydrazone (HPKIH) and thiosemicarbazone (HDpT) ligands. Indeed, the present series of compounds may be viewed as a hybrid of these latter two groups.[32,33,40] While some of the thiohydrazone analogues presented in this work have been previously synthesized,[43−47] their biological effects in terms of Fe chelation efficacy or anti-proliferative activity have not been examined. This was crucial to assess because of the potent antiproliferative effects of their related aroylhydrazone and thiosemicarbazone analogues.[32,33,40]

Synthesis of the thiohydrazone analogues involved Schiff base condensation reactions between thiobenzhydrazide and the appropriate aldehyde or ketone, as reported for the related aroylhydrazone (HPKIH) and thiosemicarbazone (HDpT) analogues.[33,38] In this case though, the thiobenzoyl hydrazones were more reactive and interconverted between various forms. The origin of the reactivity is thione/thiolene tautomerism (Figure 2), which is much more relevant here than in the chemistry of the corresponding hydrazones or thiosemicarbazones.

Recrystallization of the thiohydrazone Schiff base H_2STBH from hot ethanol yielded an oxidized azine disulfide dimer. A view of this molecule is shown in Figure 3A, where its crystallographic C_2 symmetry is apparent. The C8−N2 (double) and C8−S1 (single) bonds are consistent with azine disulfide formation, which "locks in" the thiolene tautomeric form that must have preceded dimerization.

As no oxidant was added during recrystallization of H_2STBH, dioxygen in the atmosphere must be responsible for the reaction. The initially isolated (noncrystalline) product is evidently a monomer, as shown by MS and NMR (see Experimental Procedures). None of the other ligands studied here were as susceptible to oxidation, and it should be noted that only the well characterized monomer of H_2STBH was examined for Fe chelation efficacy (see below). The rate of the oxidation reaction is not known, but the compound crystallographically characterized is distinguishable from its monomeric precursor. The rate of redox interconversion between pyridine thiones and disulfides has been shown to be dependent on a number of factors, including solvent, concentration, and exposure to UV light.[48]

In its monomeric form, H_2STBH has been reported[47] to exist in solution as a 1:1 mixture of *E*/*Z* isomers (according to the substituents attached to the C═N bond), and this was confirmed in the present study. In this case, two signals were evident in the ^{1}H NMR for each NH and OH proton, with the more deshielded pair arising from intramolecular H-bonding between the OH donor and N═C acceptor in the *Z* isomer. In addition, we showed that the ESI-MS spectrum of the original Schiff base prior to recrystallization was consistent with H_2STBH.

Previous studies have reported similar findings with other thione compounds, with a solvent- and temperature-dependent

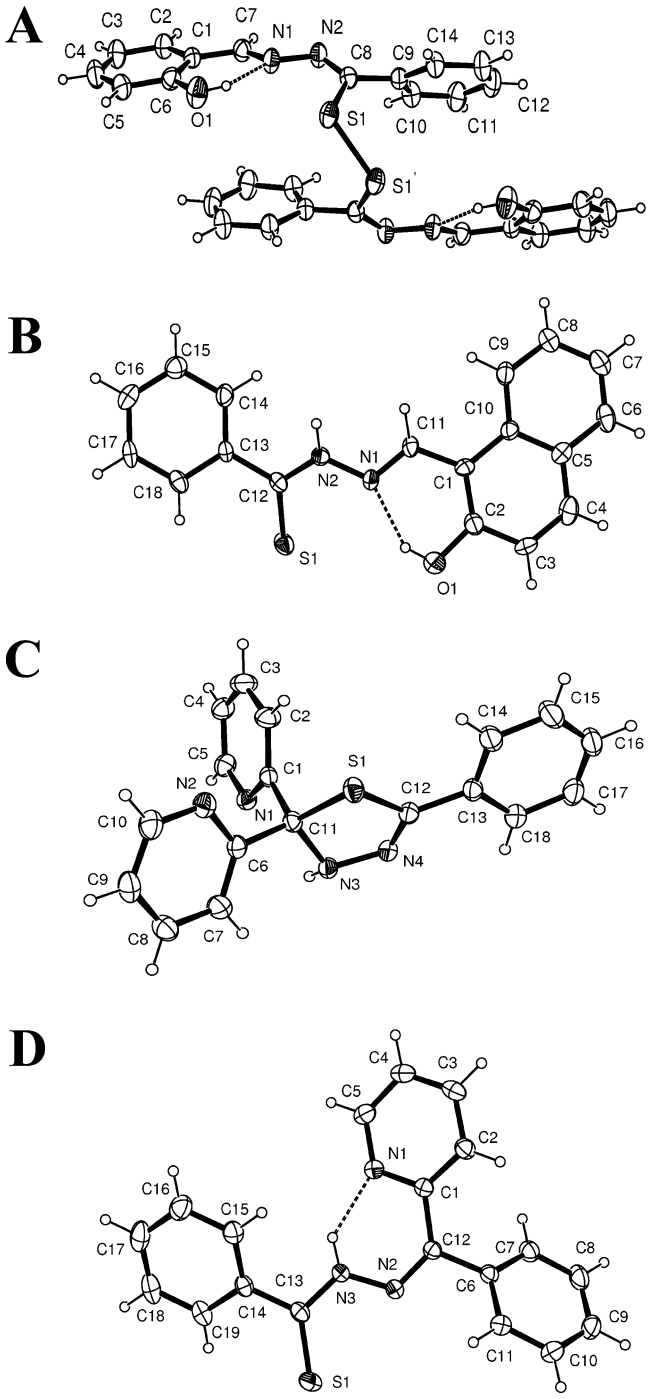

Figure 3. ORTEP diagrams of the (A) azine disulfide derivative of H_2STBH, (B) H_2NTBH, (C) cyclized derivative of HPKTBH, and (D) HBPTBH (30% probability ellipsoids shown).

reversible monomer−dimer transformation being evident, although the origin of the reductant required to cleave the S−S bond has not been established.[48−51] More significantly, other dimerized disulfide products have been observed to reverse back to the monomer in water.[49−51]

The oxidized azine disulfide (Figure 3A) would be a much less effective Fe chelator than its monomer because of steric effects and also the loss of nucleophilicity of the S-donor due to disulfide formation. Hence, the biological studies only used the well-characterized monomer. The considerable biological activity described below for H_2STBH in terms of Fe chelation efficacy (see Biological Studies), appears attributable to the original tridentate monomer being present in aqueous solution.

Indeed, maintenance of the tridentate donor set of this class of ligands is critical for effective Fe-binding, as its disruption is known to lead to marked inhibition of Fe chelation efficacy.[32]

We acquired X-ray quality crystals of H_2NTBH (Figure 3B) directly from the ethanolic reaction mixture without recrystallization. The synthesis and NMR (in DMSO-d_6) of H_2NTBH have been previously reported[43] in which a 10:1 mixture of the *E*/*Z* isomers was evident in solution, and we see a similar equilibrium here in the same solvent. The crystal structure of H_2NTBH closely resembles that of its hydrazone counterpart, 2-hydroxy-1-naphthaldehyde isonicotinoyl hydrazone (H_2NIH; Figure 1A),[52] containing an intramolecular H-bond between the hydroxyl proton and the imine nitrogen with an intramolecular N····H distance of 1.85 Å. The formation of this H-bond stabilizes the *E* isomer in which the *O*,*N*,*S*-donor atoms are preorganized in the conformation necessary for Fe complexation and thus biological activity.

We also isolated a cyclized dihydrothiadiazole derivative of HPKTBH, as confirmed by X-ray crystallography (Figure 3C). As mentioned previously, the formation of the thiolene tautomer of the thiohydrazone raises the nucleophilicity of the S-atom, which then attacks the imine C═N bond with accompanying proton transfer. It is known that dihydrothiadiazoles may equilibrate with their Schiff base precursors in solution,[53−55] thus enabling them to act as metal ion chelators.[56,57] This point is important to consider and suggests that the biological activity of these ligands described below is actually due to a similar reversible interconversion. This reaction leads to the noncyclic tridentate ligand which then acts as a biologically effective Fe chelator.

The crystal structure of HBPTBH, which was recrystallized from dichloromethane/hexane, revealed the original Schiff base (Figure 3D). The ^{13}C NMR of the original sample of HBPTBH (before recrystallization) indicated that the compound was, like its dipyridylketone analogue, HPKTBH, present in its dihydrothiadiazole form. A resonance at 95 ppm is once again apparent and indicative of a saturated C-atom in place of the C═N signal around 145 ppm.[38] It appears that these two pyridylketone derivatives are more susceptible to cyclization than the thiobenzoyl hydrazones derived from salicylaldehyde or 2-hydroxy-1-naphthaldehyde, as no cyclic derivatives of either H_2STBH or H_2NTBH were identified.

Synthesis of the Thiohydrazone Fe Complexes. Synthesis of the Fe complexes of the thiohydrazones was an important step in confirming their ability to bind Fe as tridentate ligands. Indeed, this was crucial, considering the identification of the azine disulfide dimer of H_2STBH (Figure 3A) and a cyclized dihydrothiadiazole form of HPKTBH (Figure 3C) that would be poor chelators and could not explain their high Fe chelation efficacy described below.

The ferrous complexes of H_2STBH and H_2NTBH were obtained regardless of whether a ferrous or ferric salt was used in their synthesis. Moreover, in each case, a 1:2 Fe^{II}/ligand complex was identified by elemental analysis and MS (see Experimental Procedures). The ferric complex of H_2PTBH was readily prepared by the addition of $Fe(ClO_4)_3 \cdot 6H_2O$ to the ligand in acetonitrile. The lack of a counter ion, namely, perchlorate, as determined by microanalysis and IR, suggested that both phenolic groups and a thioamide moiety were deprotonated to form a charge neutral *bis* complex. The same combination of singly and doubly deprotonated ligands was found in the ferric complex Fe(HNIH)(NIH) (see Figure 1A).[52]

The ferrous complexes of both HPKTBH and HBPTBH were readily prepared by the addition of the ferrous salt to the ligand under nitrogen. As previously mentioned, cyclic dihydrothiadiazole analogues have been shown to form metal complexes where the ligand is able to revert to its acyclic Schiff base form.[56,57] The ^{1}H NMR spectra of these ferrous complexes were obtained showing sharp peaks indicating that their Fe complexes were in the low-spin state in solution. Elemental analysis indicated that the compounds were charge neutral 1:2 Fe^{II}/ligand complexes without any counter ions, which requires both ligands to be bound in their singly deprotonated form. Considering this, charge neutrality is important in terms of the diffusion of the ligand through biological membranes and its efflux as an Fe complex from cells.[1,58]

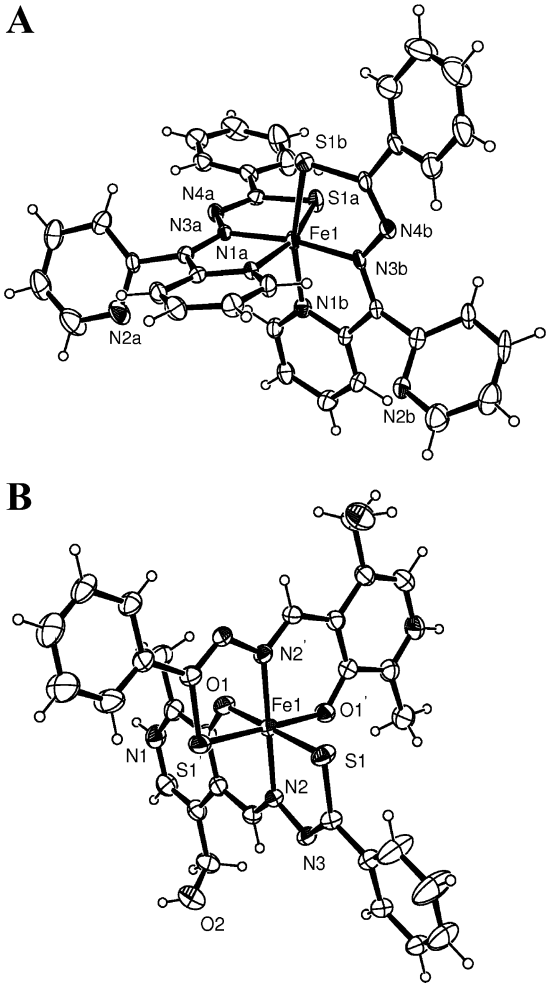

Figure 4. ORTEP representations of (A) $Fe^{II}(PKTBH)_2$ (30% probability ellipsoids shown). Selected bond lengths (Å) N(1A)-Fe(1) 1.979(6); N(1B)-Fe(1) 1.969(6); N(3A)-Fe(1) 1.912(6); N(3B)-Fe(1) 1.887(6); S(1A)-Fe(1) 2.274(3); S(1B)-Fe(1) 2.291(3) and (B) $[Fe^{III}(HPTBH)_2]^+$ (30% probability ellipsoids shown) are shown. Selected bond lengths (Å) O(1)-Fe(1) 1.917(3); N(2)-Fe(1) 1.920(3); and S(1)-Fe(1) 2.226(1). Primes denote symmetry related atoms ($-x$, y, $-z+1/2$).

The crystal structure of $Fe(PKTBH)_2$ was determined (Figure 4A) and confirmed the data described above. The coordination sphere comprised a distorted octahedral *cis*-N_4S_2 set of donor atoms. The two ligands are orthogonal and define a meridional isomeric configuration, which is dictated by the planarity of the ligand backbone. The coordinate bonds are consistent with low spin Fe^{II} with the shortest bonds being the pair of Fe-N3A,B bonds. This axial compression is a consistent feature in the structures of all complexes of tridentate hydrazones that we have reported previously.[38,52,59,60]

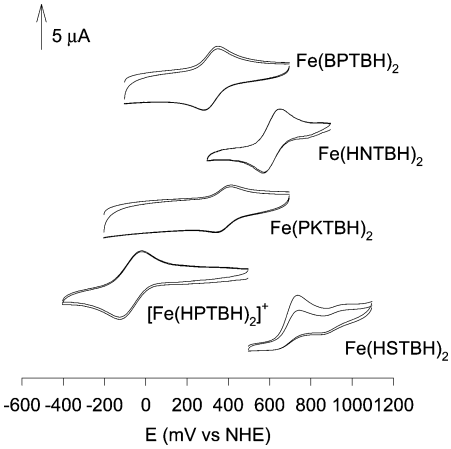

Figure 5. Cyclic voltammograms of all Fe complexes examined in this study. Sweep rate 100 mVs^{-1}, solvent 70:30 DMF/H_2O with 0.1 M $NaClO_4$.

The Fe^{III} complex $[Fe(HPTBH)_2]Cl\cdot 2H_2O$ was also characterized structurally (Figure 4B). The complex resides on a 2-fold axis as does the single chloride counter ion. A water molecule is disordered over four different positions. The Fe is six-coordinate with an $Fe^{III}O_2N_2S_2$ coordination sphere. As expected, the phenolic protons are lost upon coordination of the ligand to Fe as are the amide protons on each ligand. However, each ligand is only a monoanion, as a proton is found on each pyridoxal ring N-atom where it donates an H-bond to the chloride counterion. The Fe−O bond lengths are shorter than the Fe−N bonds, which reflect the preference of the higher oxidation state for the harder phenolic O-donor atoms. Interestingly, the Fe−O and Fe−N bond lengths in $[Fe(HPTBH)_2]^+$ are much shorter than those found in the high-spin Fe^{III} relative [Fe(NIH)(HNIH)] that we reported previously.[52] Clearly, the introduction of an S-donor (thiohydrazone) in place of an O-donor (hydrazone) switches the Fe^{III} ground state from high spin to low spin. Again, the X-ray crystal structure of the Fe complex of this class of ligands demonstrates their ability to act as tridentate chelators.

In summary, all of the thiohydrazone chelators acted as tridentate ligands to bind Fe. This is important to note considering the identification of the azine disulfide dimer of H_2STBH and the cyclized dihydrothiadiazole form of HPKTBH. This conforms with the idea that multiple species of these chelators exist in solution and agrees with previous studies examining other thiohydrazones.[49−51,56,57] Moreover, it is the monomeric, noncyclic form of the ligand that acts to effectively bind Fe.

Electrochemistry of the Fe Complexes. The redox potentials of all complexes were examined with cyclic voltammetry (Figure 5). The two pyridyl coordinated complexes $Fe(PKTBH)_2$ and $Fe(BPTBH)_2$ yielded reversible $Fe^{III/II}$ redox couples in aqueous solution (pH 7) at +383 and +328 mV versus NHE, respectively. The complexes with phenolic O-donors were quite different from each other. A reversible couple was obtained from $Fe(HNTBH)_2$ (+608 mV), but an irreversible anodic wave was obtained for $Fe(HSTBH)_2$ (E_{pa} +740 mV). Given the similarity in coordination spheres, the difference in reversibility is probably related to the higher potential Fe^{III} complex being rapidly reduced by water, while the lower potential naphthaldehyde analogue is stable on the voltammetric time scale. The $Fe(HSTBH)_2$ complex shows a low potential single electron reversible wave that was found at −520 mV, which may be a ligand-centered reduction. Finally, the pyridoxal analogue $[Fe(HPTBH)_2]^+$ showed the lowest redox potential (−76 mV), which is consistent with its isolation as an Fe^{III} complex.

Cyclic voltammetry was also essential in assigning the oxidation state of the products as isolated. This was established by initiating the voltammetric sweep from both the positive and negative directions with no equilibration time. These results indicate that starting the voltammetric sweep in the cathodic direction is accompanied by an immediate large anodic current when ferrous complexes are present (indicative of the immediate oxidation of the bulk ferrous complex). By contrast, no initial current was seen when the sweep was initiated in the anodic direction. Hence, H_2STBH and H_2NTBH, which have an *O,N,S*-donor system, clearly have a preference for Fe^{II} over Fe^{III}. In contrast, their oxygen-containing analogues, H_2SBH and H_2NBH, which possess a *O,N,O*-donor atom system, belong to the aroylhydrazone group of ligands that readily form Fe^{III} complexes.[52]

These results suggest that the ability of the Fe complexes of HPKTBH and HBPTBH to redox cycle and facilitate the production of ROS may play an integral role in their potent anti-proliferative activity discussed below.

Biological Studies. Anti-Proliferative Activity of the Ligands Against Tumor Cells. The effect of the replacement of S for O in the ligating sites on the anti-proliferative activity of the chelators was examined using human SK-N-MC neuroepithelioma cells. This cell line was used as the effect of Fe chelators on their growth is well characterized,[29,32,41,61,62] enabling comparison to previous studies. The new thiohydrazone analogues were examined in comparison to a number of controls, including (1) their corresponding oxygen parent ligands;[30,38,41] (2) desferrioxamine (DFO; Figure 1A), which is used for the treatment of Fe overload disease;[5] (3) the chelator, 3-AP (Figure 1A), which was designed specifically as an anti-tumor agent;[24,63] (4) the ligand, H_2NIH (Figure 1A), which has moderate anti-proliferative activity;[61,62] and (5) the Fe chelator with potent anti-tumor activity, di-2-pyridylketone 4,4-dimethyl-3-thiosemicarbazone (HDp44mT; Figure 1A).[32,33,40]

The replacement of the carbonyl oxygen donor atom with sulfur resulted in mixed effects on the anti-proliferative activity of these thiohydrazone ligands depending on their donor set (Table 2). Interestingly, those ligands using the *O,N,S*-donor set, such as H_2PTBH, H_2STBH, and H_2NTBH, demonstrated anti-proliferative effects that were approximately 2−8-fold lower than that of their corresponding *O,N,O* parent ligands, H_2PBH, H_2SBH, and H_2NBH, respectively (Table 2). In each case, the parent oxygen ligand was found to have significantly ($p < 0.0001$) greater anti-tumor effects than its sulfur analogue.

However, those chelators utilizing the *N,N,S*-donor atom set, including HPKTBH ($IC_{50} = 0.012\ \mu M$; Table 2) and HBPTBH ($IC_{50} = 0.011\ \mu M$; Table 2), were found to show a significant ($p < 0.0001$) increase in anti-proliferative activity than their corresponding *N,N,O* ligands, HPKBH and HBPBH, respectively (Table 2). In fact, these thiohydrazone analogues were found to have anti-proliferative effects between 103−134-fold greater than their corresponding oxygen ligands, making these thiohydrazone chelators comparably as active as other thiosemicarbazones such as the HDpT series developed by our group.[32,33,40] Therefore, both HPKTBH and HBPTBH have potential as anti-tumor agents and deserve further attention.

While the control, DFO, exhibited significantly ($p < 0.0005$) greater or comparable anti-proliferative activity to H_2PTBH and H_2STBH, respectively, all other thiohydrazone analogues were significantly ($p < 0.05$) more potent (Table 2). Generally, while DFO shows some anti-proliferative activity both *in vitro* and *in vivo*, its potency is limited because of its poor membrane

Table 1. Crystal Data

	H_2STBH disulfide	H_2NTBH	cyclized HPKTBH	HBPTBH	Fe(PKTBH)$_2$	[Fe(HPTBH)$_2$]Cl·H_2O
formula	$C_{28}H_{22}N_4O_2S_2$	$C_{18}H_{14}N_2OS$	$C_{18}H_{14}N_4S$	$C_{19}H_{15}N_3S$	$C_{36}H_{26}FeN_8S_2$	$C_{30}H_{32}ClFeN_6O_6S_2$
mol. wt	510.62	306.37	318.39	317.40	690.62	728.04
crystal system	monoclinic	orthorhombic	monoclinic	monoclinic	monoclinic	monoclinic
a (Å)	28.520(5)	8.4581(8)	11.766(2)	8.606(1)	10.544(5)	18.629(2)
b (Å)	6.2535(3)	17.625(2)	8.1669(6)	16.416(3)	27.81(1)	17.260(2)
c (Å)	16.055(3)	19.880(3)	17.109(4)	11.231(4)	11.469(7)	12.119(2)
β (deg)	120.71(1)		109.23(1)	93.84(2)	106.12(3)	109.04(1)
V (Å^3)	2461.8(6)	2963.6(6)	1552.3(5)	1583.1(7)	3231(3)	3683.5(8)
T (K)	293	293	293	293	293	293
Z	4	8	4	4	4	4
space group	*C*2/*c*	*P c a b*	*P*2$_1$/*n*	*P*2$_1$/*c*	*P*2$_1$/*n*	*C*2/*c*
μ (mm^{-1})	0.251	0.221	0.213	0.207	0.636	0.642
indep. refs (R_{int})	2171 (0.0211)	2585 (0.1218)	2722 (0.0089)	2768 (0.0208)	5672 (0.0835)	3237 (0.0359)
R_1 (obs. data)	0.0380	0.0643	0.0285	0.0335	0.0684	0.0529
wR_2 (all data)	0.1113	0.1237	0.0794	0.0905	0.2266	0.1898
CCDC no.	653022	653023	653024	653025	653026	660701

Table 2. IC_{50} (μM) Values of the Thiohydrazones and their Fe Complexes at Inhibiting the Growth of SK-N-MC Neuroepithelioma and Normal MCR-5 Fibroblast Cells[a]

ligand	IC_{50} (μM) of ligand against SK-N-MC neuroepithelioma cells	*p* value (O vs S)	IC_{50} (μM) of Fe complex against SK-N-MC neuroepithelioma cells	*p* value (ligand vs Fe complex)	IC_{50} (μM) of ligand against MRC-5 fibroblast cells	*p* value (SK-N-MC vs MRC-5 cells)
DFO	14.22 ± 7.54				> 25[b]	
3-AP	0.54 ± 0.13				ND	
H_2NIH	0.59 ± 0.23				> 25[b]	
HDp44mT	0.002 ± 0.001				> 25[b]	
H_2PBH	31.82 ± 0.16					
H_2PTBH	58.25 ± 2.39	$p < 0.001$	> 80	$p < 0.001$	> 80	$p < 0.001$
H_2SBH	3.23 ± 0.26					
H_2STBH	24.47 ± 4.84	$p < 0.001$	> 80	$p < 0.001$	57.01 ± 16.36	$p < 0.01$
H_2NBH	0.99 ± 0.01					
H_2NTBH	2.53 ± 0.05	$p < 0.001$	36.58 ± 1.21	$p < 0.001$	3.89 ± 0.29	$p < 0.001$
HPKBH	1.24 ± 0.07					
HPKTBH	0.012 ± 0.001	$p < 0.001$	0.14 ± 0.01	$p < 0.001$	0.75 ± 0.05	$p < 0.001$
HBPBH	1.47 ± 0.05					
HBPTBH	0.011 ± 0.001	$p < 0.001$	3.60 ± 0.80	$p < 0.001$	0.53 ± 0.18	$p < 0.05$

[a] Comparable data for DFO, 3-AP, H_2NIH, and HDp44mT are also shown. The *p* values were determined using Student's *t*-test, and we compared the anti-proliferative activity of the parent oxygen chelator (O) to the thiohydrazone analogue (S) or Fe complex or the anti-proliferative activity of the thiohydrazones in SK-N-MC vs MRC-5 cells. The results are the mean ± SD (3 experiments). ND indicates not determined. [b] IC_{50} data determined previously.[32]

permeability.[5] In fact, ligands that have comparable effects to DFO would not be considered as effective anti-tumor agents. The control chelators, 3-AP and H_2NIH, demonstrated significantly ($p < 0.0005$) greater efficacy than all thiohydrazone analogues except HPKTBH and HBPTBH. The ligand HDp44mT, which possesses potent anti-tumor activity,[40] was found to have greater anti-proliferative effects ($IC_{50} = 0.002$ μM) than all the thiohydrazone analogues examined.

Anti-Proliferative Activity of the Fe Complexes against Tumor Cells. Various studies performed previously have shown that some Fe complexes demonstrate increased anti-proliferative effects compared to those of their free ligands.[60,62,64,65] We examined the cytotoxicity of the synthesized thiohydrazone Fe complexes on the SK-N-MC neuroepithelioma cell line.

All thiohydrazone Fe complexes demonstrated significantly ($p < 0.001$) decreased anti-proliferative effects compared to those of the free ligand (Table 2). The Fe complexes of both H_2PTBH and H_2STBH showed little activity ($IC_{50} > 80$ μM), while the other Fe complexes, $Fe^{II}(HNTBH)_2$, $Fe^{II}(PKTBH)_2$, and $Fe^{II}(BPTBH)_2$, were found to be 12- to 343-fold less effective than the free thiohydrazone ligand (Table 2).

Anti-Proliferative Activity of the Ligands against Normal Cells. In order for an Fe chelator to be considered as a therapeutic agent, it must demonstrate selective anti-proliferative activity, targeting cancer cells while leaving normal cells relatively unharmed. Therefore, the anti-proliferative activity of the thiohydrazone analogues was examined in mortal MRC-5 fibroblasts (Table 2). All thiohydrazone analogues demonstrated a marked and significant ($p < 0.05$) decrease in anti-proliferative activity in normal cells in comparison with neoplastic cells. In fact, the most potent thiohydrazone analogues assessed in this study, HPKTBH and HBPTBH, exhibited a 50−63-fold decrease in anti-proliferative effects in mortal cells. These results suggest an appreciable therapeutic index, targeting cancer cells over normal cells.

Cellular Fe Efflux. In an effort to determine the factors mediating the changes in anti-proliferative activity between the sulfur analogues and their parent oxygen chelators, initial studies examined the ability of these ligands at mobilizing intracellular ^{59}Fe from prelabeled SK-N-MC cells (Figure 6A). This cell line was examined as its Fe metabolism is well characterized, and the effects of other chelators on inducing Fe efflux and preventing Fe uptake have been reported previously.[32,41,61,63,66] These ligands were compared to a number of positive controls including H_2PIH (Figure 1A), H_2NIH, HDp44mT, and DFO, which have been extensively examined.[32,41,61,63,66]

As previously shown,[33,35] the positive controls, H_2PIH, H_2NIH, and HDp44mT, showed marked ^{59}Fe-mobilizing efficacy, releasing 44−49% of cellular ^{59}Fe (Figure 6A). In comparison, the highly hydrophilic chelator, DFO, demonstrated limited ^{59}Fe mobilization activity as reported previously,[66] releasing 17 ± 1% of cellular ^{59}Fe, while the control medium resulted in only 5 ± 1% of cellular ^{59}Fe release (Figure 6A).

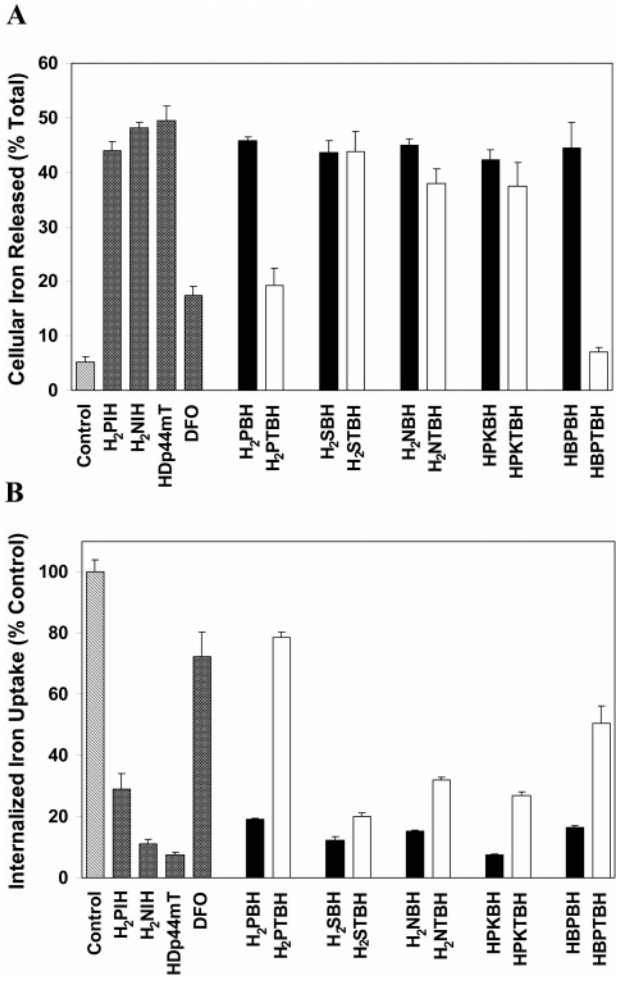

Figure 6. Effect of the thiohydrazone analogues in comparison with their parent oxygen analogue on (A) ^{59}Fe mobilization from prelabeled SK-N-MC neuroepithelioma cells and (B) ^{59}Fe uptake from ^{59}Fe-transferrin (^{59}Fe-Tf) by SK-N-MC neuroepithelioma cells. Results are the mean ± SD of 3 experiments with 3 determinations in each experiment.

The thiohydrazone analogues, H_2STBH, H_2NTBH, and HPKTBH demonstrated high ^{59}Fe-mobilizing efficacy, releasing 37−44% of cellular ^{59}Fe (Figure 6A). In contrast to H_2STBH and HPKTBH that showed comparable ^{59}Fe mobilization activity to their parent oxygen analogues, the majority of thiohydrazone analogues were significantly ($p < 0.01$) less effective at releasing cellular ^{59}Fe when compared with their corresponding oxygen ligands.

The high ^{59}Fe-mobilizing activity of H_2STBH and HPKTBH was found to be comparable to that of H_2PIH, while all other thiohydrazone analogues demonstrated significantly ($p < 0.05$) reduced efficacy in releasing cellular ^{59}Fe. Of the thiohydrazone analogues, only H_2STBH demonstrated comparable ^{59}Fe-mobilizing efficacy to that of H_2NIH and HDp44mT. All other thiohydrazone analogues were significantly ($p < 0.05$) less effective than these two positive controls. The majority of thiohydrazone analogues demonstrated significantly ($p < 0.001$) greater ^{59}Fe-mobilizing activity than DFO. However, it is of interest that despite the high anti-proliferative activity of HBPTBH, this ligand exhibited significantly ($p < 0.001$) reduced efficacy in mobilizing cellular ^{59}Fe than DFO. The reason for the low Fe chelation efficacy of HBPTBH is unclear at present.

Inhibition of Cellular ^{59}Fe Uptake from ^{59}Fe-Transferrin. The ability of the thiohydrazone chelators to inhibit ^{59}Fe uptake from the Fe transport protein, ^{59}Fe-Tf, was also assessed using the SK-N-MC cell line (Figure 6B). This was critical to determine, as anti-proliferative activity relies, in part, on the ability of a chelator to mobilize cellular Fe as well as to prevent Fe uptake from Tf.[41] As previously described,[32,41] the positive controls, H_2PIH, H_2NIH, and HDp44mT, were very effective at inhibiting ^{59}Fe uptake from ^{59}Fe-Tf, reducing it to 29 ± 5%, 11 ± 2%, and 8 ± 1% of the control, respectively (Figure 6B). However, the hydrophilic chelator, DFO, was only able to inhibit ^{59}Fe uptake to 72 ± 8% of the control (Figure 6B), in agreement with previous work.[35,61]

The thiohydrazone analogues that were effective at mobilizing cellular ^{59}Fe (Figure 6A) also markedly inhibited ^{59}Fe uptake from ^{59}Fe-Tf. Indeed, H_2STBH, H_2NTBH, and HPKTBH effectively reduced ^{59}Fe uptake from ^{59}Fe-Tf to 20−32% of the control (Figure 6B). Interestingly, each sulfur analogue was significantly ($p < 0.001$) less effective than its corresponding oxygen analogue at preventing the uptake of ^{59}Fe from Tf. This observation, in part, may explain the decreased anti-proliferative activity of H_2PTBH, H_2STBH, and H_2NTBH in comparison with that of their oxygen-containing counterparts (Table 2).

The thiohydrazone analogues, H_2STBH, H_2NTBH, and HPKTBH, resulted in comparable inhibition of ^{59}Fe uptake from ^{59}Fe-Tf as the highly effective ligand, H_2PIH (Figure 6B). This suggests easy access to intracellular Fe pools and effective Fe chelation. The high Fe-chelation efficacy of HPKTBH indicates that while this ligand was isolated in the cyclic form (Figure 3C), it is probable that the acyclic, tridentate ligand is involved in Fe chelation. These observations substantiate the chemical evidence already discussed, indicating that this form exists in equilibrium with the effective acyclic chelator.

All thiohydrazone analogues were significantly ($p < 0.005$) less effective than the positive controls, H_2NIH and HDp44mT. However, all thiohydrazone analogues, besides H_2PTBH, were significantly more effective than DFO at preventing ^{59}Fe uptake (Figure 6B).

Ascorbate Oxidation by the Fe Complexes. In order to determine whether redox cycling played a role in the anti-proliferative activity of the thiohydrazone analogues, we examined the ability of their Fe complexes to mediate the oxidation of the physiological substrate, namely, ascorbate, using established methodology.[33] In these experiments, the oxidation of ascorbate mediated by the Fe complexes of the thiohydrazone analogues was compared to that of their parent oxygen ligands (Figure 7). As a positive control, the ability of the Fe complex of EDTA to oxidize ascorbate was assessed.[38,67,68]

In these redox experiments, the results were expressed in terms of iron-binding equivalents (IBE) because of the different denticity of the ligands used, that is, the hexadentate ligand, EDTA, forms a 1:1 Fe/ligand complex, while all other ligands examined are tridentate, forming 1:2 Fe/ligand complexes.[41,68] Three IBEs were chosen, namely, 0.1, 1, and 3, to assess the redox activity of the thiohydrazones. An IBE of 0.1 represents an excess of Fe, where 1 hexadentate chelator or 2 tridentate chelator molecules are in the presence of 10 Fe ions. An IBE of 1 results in the complete filling of the coordination sphere, while an IBE of 3 represents an excess of ligand to Fe, where 3 hexadentate or 6 tridentate ligands are in the presence of 1 Fe ion.

In agreement with previous studies,[33,38,39,67,68] EDTA was able to increase the oxidation of ascorbate to 316% and 317% of the control at IBEs of 1 and 3, respectively, while less activity was evident at an IBE of 0.1 (Figure 7). In this study, EDTA was found to be significantly ($p < 0.005$) more effective at

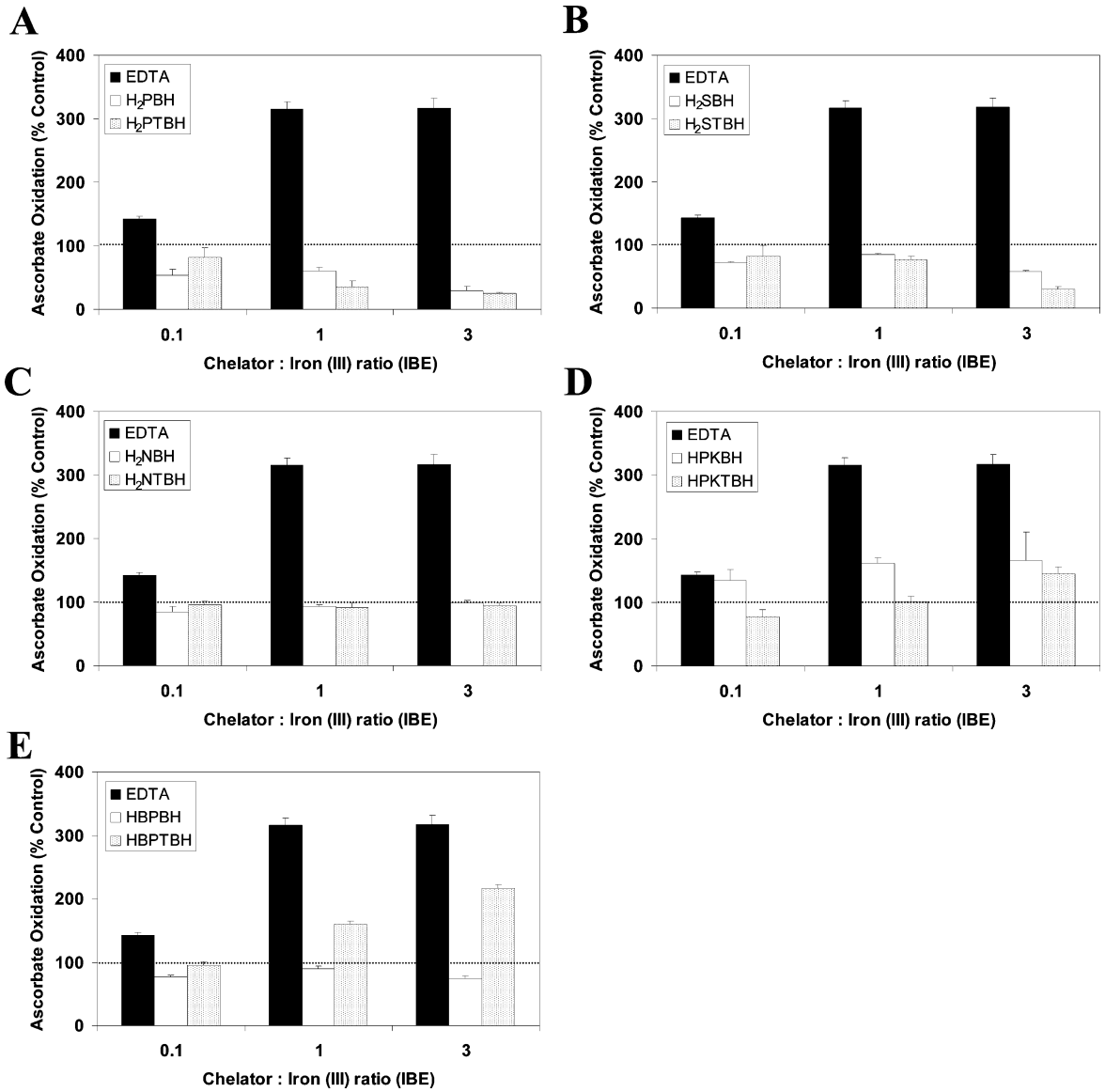

Figure 7. Effect of the Fe complexes of the thiohydrazone analogues and their corresponding oxygen ligands on ascorbate oxidation. Chelators at iron-binding equivalent (IBE) ratios of 0.1, 1, and 3 were incubated in the presence of Fe^{III} (10 μM) and ascorbate (100 μM). The UV absorbance at 265 nm was recorded after 10 and 40 min and the difference between the time points calculated. Comparison of the positive control EDTA with (A) H_2PBH and H_2PTBH; (B) H_2SBH and H_2STBH; (C) H_2NBH and H_2NTBH; (D) HPKBH and HPKTBH; and (E) HBPBH and HBPTBH is shown. Results are the mean ± SD (3 experiments).

increasing ascorbate oxidation in comparison to all thiohydrazone analogues at IBEs of 1 and 3.

Substitution of the donor carbonyl oxygen with a sulfur atom had varied results on the ability of the thiohydrazone Fe complexes to mediate the oxidation of ascorbate (Figure 7). Those ligands utilizing the *O*,*N*,*S*-donor atoms, that is, H_2PTBH (Figure 7A), H_2STBH (Figure 7B), and H_2NTBH (Figure 7C), bound Fe and either prevented or did not markedly affect the oxidation of ascorbate in comparison to the control. In fact, the Fe complexes of these thiohydrazone analogues were found to mediate comparable levels of ascorbate oxidation to that of their parent oxygen ligands at all IBEs (Figure 7A−C). Only H_2STBH (Figure 7B) was found to significantly ($p < 0.005$) decrease levels of ascorbate oxidation in comparison to its parent oxygen ligand, H_2SBH, at an IBE of 3. This demonstrated that H_2STBH had even greater protective effects on ascorbate oxidation than its parent oxygen analogue during this assay.

In contrast to the thiohydrazones described above, the *N*,*N*,*S*-ligands, HPKTBH (Figure 7D) and HBPTBH (Figure 7E), were found to stimulate the Fe^{III}-mediated oxidation of ascorbate to 145% and 217% of the control at an IBE of 3, respectively. HPKTBH showed comparable activity to its oxygen ligand, HPKBH, at mediating Fe^{III}-catalyzed ascorbate oxidation at an IBE of 3. However, HBPTBH was found to significantly ($p < 0.0001$) increase the oxidation of ascorbate in comparison to HBPBH at all IBEs (Figure 7E). This redox activity of HBPTBH may be particularly significant in terms of explaining its high anti-proliferative efficacy, as its ability to mobilize cellular ^{59}Fe and prevent ^{59}Fe uptake were not marked (Figure 6). These results suggest that redox cycling may play an important role in the potent anti-proliferative activity of HPKTBH and HBPTBH, resulting in ROS generation and oxidative damage to cells. This work is in agreement with previous studies of other *N*,*N*,*S*-ligands, such as the HDpT series of chelators, in which redox cycling was found to be an important factor contributing to their anti-proliferative activity.[33,35]

Benzoate Hydroxylation. As an additional measurement of redox activity, the benzoate hydroxylation assay was employed

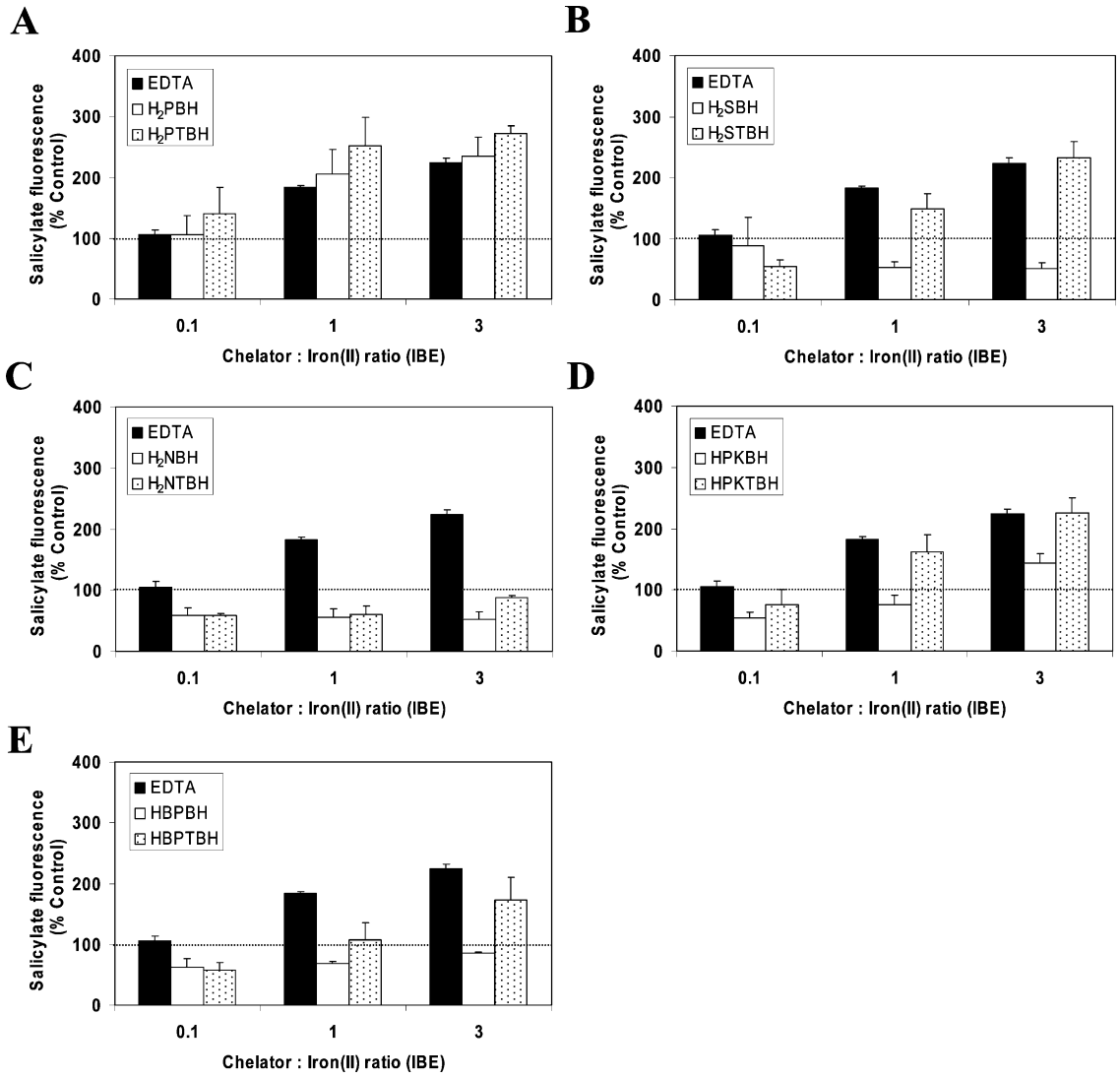

Figure 8. Effect of various Fe chelators on the hydroxylation of benzoate in the presence of Fe^{II} and hydrogen peroxide. Chelators at iron-binding equivalent (IBE) ratios of 0.1, 1, and 3 were incubated for 1 h at room temperature in the presence of Fe^{II} (30 μM), hydrogen peroxide (5 mM), and benzoate (1 mM). The fluorescence of hydroxylated benzoate was measured at 308 nm excitation and 410 nm emission. Comparison of the positive control EDTA with (A) H_2PBH and H_2PTBH; (B) H_2SBH and H_2STBH; (C) H_2NBH and H_2NTBH; (D) HPKBH and HPKTBH; and (E) HBPBH and HBPTBH is shown. Results are the mean ± SD (3 experiments).

to investigate the redox cycling capabilities of the Fe^{II} complexes of the thiohydrazone analogues (Figure 8). This assay measures the ability of the Fe complexes to catalyze the breakdown of hydrogen peroxide, generating hydroxyl radicals that subsequently hydroxylate benzoate.[35,68]

In the presence of Fe^{II}, the positive control, EDTA, was able to enhance the hydroxylation of benzoate to 183% and 224% of the control at IBEs of 1 and 3, respectively (Figure 8). This ability to promote benzoate hydroxylation at these IBEs was in agreement with previous studies.[35,68] Interestingly, the ability of the Fe^{II} complexes of the thiohydrazone analogues to promote benzoate hydroxylation varied (Figure 8A−E). Of the thiohydrazones, H_2NTBH (Figure 8C) demonstrated protective effects, reducing the hydroxylation of benzoate to 89% of the control at an IBE of 3. In contrast, all other thiohydrazone analogues were found to enhance benzoate hydroxylation to 172−273% of the control at an IBE of 3 (Figure 8).

H_2PTBH was the only sulfur analogue to show benzoate hydroxylation effects comparable to that of its oxygen analogue, H_2PBH, at IBEs of 1 and 3, markedly increasing the hydroxylation of benzoate (Figure 8A). In fact, both compounds showed activity comparable to that of EDTA at an IBE of 3. It is notable that $[Fe(HPTBH)_2]^+$ has the lowest redox potential of the current series and that both H_2PTBH and H_2PBH showed protective effects during the ascorbate oxidation assay. Likewise, the structurally related aroylhydrazone Fe chelator, H_2PIH, was previously observed to stimulate benzoate hydroxylation in the presence of Fe^{II}, while having little effect on the Fe^{III}-mediated oxidation of ascorbate.[68] Thus, the benzoate hydroxylation reaction was thought to be facilitated by the strong preference of H_2PIH for Fe^{III} over Fe^{II}.[68] The current results suggest that H_2PTBH and H_2PBH may also behave in this manner, driving the hydroxylation of benzoate by their preference for Fe^{III}.

In the presence of Fe^{II}, H_2STBH was also found to enhance the hydroxylation of benzoate at IBEs of 1 and 3, significantly ($p < 0.01$) more so than its parent oxygen chelator, H_2SBH, which demonstrated protective effects (Figure 8B). In fact, the levels of benzoate hydroxylation mediated by the Fe^{II} complex of H_2STBH at IBEs of 1 and 3 were comparable to that of EDTA. It is probable that H_2STBH acts in a manner similar to that of the HPKIH series of chelators that bind Fe^{II} and act as poor oxidants of ascorbate, but exhibit moderate ability to mediate Fe^{II}-catalyzed benzoate hydroxylation.[38]

Consistent with the ascorbate oxidation results, the *N*,*N*,*S*-ligands, HPKTBH (Figure 8D) and HBPTBH (Figure 8E), were found to stimulate the Fe^{II}-mediated levels of benzoate hydroxylation to 225% and 175%, respectively, at an IBE of 3. These levels of benzoate hydroxylation were found to be comparable to that of EDTA. Additionally, the HPKTBH and HBPTBH analogues displayed significantly ($p < 0.05$) enhanced levels of benzoate hydroxylation in comparison to those of their parent oxygen analogues. These results suggest that replacement of the oxygen donor atom with sulfur leads to increased redox activity and thus the anti-proliferative efficacy of these *N*,*N*,*S* ligands. Hence, these data are in agreement with our previous work indicating that similar thiosemicarbazone ligands are redox active and that this characteristic appears important for their anti-proliferative activity.[33,35]

It is of interest to note that the redox activity in terms of benzoate hydroxylation (i.e., hydroxyl radical generation; Figure 8) of compounds that have low anti-proliferative activity, such as H_2PTBH ($IC_{50} = 58$ μM) and H_2STBH ($IC_{50} = 24$ μM), is comparable to or higher than that found for HPKTBH and HBPTBH, which demonstrate marked anti-tumor efficacy, that is, IC_{50} values of 0.012 and 0.011 μM, respectively. Critically, this could lead to a conclusion that redox activity is not a determinant of the anti-cancer effects of these compounds. However, it is clear that H_2PTBH and H_2STBH prevent ascorbate oxidation, while HPKTBH and HBPTBH facilitate oxidation of this substrate (Figure 7). Therefore, the redox activity and overall anti-tumor effects cannot be simply judged from one assay, but necessitates a complete analysis assessing electrochemical characterization, ascorbate oxidation, benzoate hydroxylation, and Fe chelation efficacy. Indeed, our previous studies clearly state that no single factor is responsible for the anti-proliferative activity of Fe chelators.[35,41]

Overall, the low anti-proliferative activity of H_2PTBH is probably at least partially explained by its low Fe chelation efficacy in comparison to more active chelators such as HPKTBH (Figure 6A and B). However, the irreversible electrochemistry and high redox potential of the Fe complex of H_2STBH could account, in part, for its low anti-proliferative effects. The high anti-tumor activity of HPKTBH can be explained by several factors including marked Fe-chelation efficacy and facile redox chemistry mediated by its low redox potential and ability to induce ascorbate oxidation and benzoate hydroxylation. Finally, for HBPTBH, its high anti-proliferative effects are thought to be induced through reversible electrochemistry and high redox activity.

Conclusions

Through the synthesis and biological evaluation of thiohydrazone Fe chelators, we have identified crucial structure−activity relationships regarding the importance of donor atom identity on marked anti-tumor activity. All of the thiohydrazone chelators were found to bind Fe as tridentate ligands and this was demonstrated by MS, elemental analysis, and X-ray crystallography. This is important to note despite the identification of the oxidized azine disulfide of H_2STBH and the cyclized dihydrothiadiazole form of HPKTBH. Collectively, our data strongly supports the hypothesis that multiple species of these chelators exist in solution and agrees with previous studies examining other thiohydrazones.[49−51,56,57] Moreover, it is the acyclic, monomeric form of these compounds that acts as an effective ligand. In fact, the disulfide dimer of H_2STBH and cyclized form of HPKTBH could not be expected to act as biologically potent Fe chelators, as disruption of tridentate binding in this general class of ligands leads to inhibition of Fe chelation activity.[32] The high Fe chelation efficacy of H_2STBH and HPKTBH in Fe uptake and mobilization studies suggests these compounds act as tridentate chelators.

The current study also demonstrated that *O*,*N*,*S*-thiohydrazones showed reduced anti-proliferative activity compared to that of their parent *O*,*N*,*O*-hydrazone analogues. This result is analogous to that seen in another study where the *O*,*N*,*S* 2-hydroxy-1-naphthaldehyde thiosemicarbazone series showed lower anti-proliferative effects than their related *O*,*N*,*O* hydrazone, H_2NIH.[29] However, the Fe complexes of those thiohydrazones utilizing the *N*,*N*,*S*-donor set demonstrated a totally reversible $Fe^{II/III}$ couple in the range accessible to intracellular oxidants and reductants. This suggests that the high anti-proliferative activity of both HPKTBH and HBPTBH are, at least in part, due to the low redox potentials of their Fe complexes, facilitating the generation of cytotoxic ROS. The ability of their Fe complexes to mediate the oxidation of ascorbate and the hydroxylation of benzoate indicate their ROS-generating capabilities. These results support the idea that the increased anti-tumor effects of the HDpT series were at least partially due to the presence of the sulfur donor atom.[33]

Collectively, this investigation highlights the importance of donor atom identity on the anti-proliferative effects of Fe chelators. In particular, the *N*,*N*,*S*-donor atom set was found to be a crucial structural feature necessary for potent anti-tumor activity.

Experimental Procedures

Synthesis. All commercial reagents were used without further purification. Desferrioxamine (DFO) was obtained from Novartis (Basel, Switzerland). 3-AP was a gift from Vion Pharmaceuticals, New Haven, CT. The precursors, *S*-(thiobenzoyl)thioglycolic acid, hydrazine hydrate, pyridoxal hydrochloride, salicylaldehyde, 2-hydroxy-1-naphthaldehyde, di-2-pyridylketone, and 2-benzoylpyridine were obtained from Sigma-Aldrich, and all solvents used were of analytical purity. The parent compounds, H_2PBH, H_2SBH, H_2NBH, HPKBH, and HBPBH, were prepared according to previously described methods.[38,69−71]

Physical Methods. ^{1}H NMR (300 MHz) spectra were acquired in the specified solvents on a Varian Gemini 300 BB NMR spectrometer. Infrared spectra were measured on a FT-IR IFS 66V spectrophotometer using an ATR (attenuated total reflectance) assembly. Mass spectra were obtained via ESI on a ThermoFinnigan TSQ 7000 spectrometer. Elemental analysis was conducted using a Carlo Erba 1106 analyzer. Cyclic voltammetry was performed using a BAS100B/W potentiostat. A glassy carbon working electrode, an aqueous Ag/AgCl reference, and Pt wire auxiliary electrode were used. All complexes were at ca. 1 mM concentration in DMF/H_2O 70:30 v/v. This solvent combination was used to ensure the solubility of these compounds. The supporting electrolyte was NaClO4 (0.1 M), and the solutions were purged with nitrogen prior to measurement. All potentials are cited versus the normal hydrogen electrode (NHE) by addition of 196 mV to the potentials measured relative to the Ag/AgCl reference.

Elemental analysis (C, H, N, S) of the ligands and complexes was performed, and the results, available as Supporting Information, were within ± 0.4% of the theoretical values, unless otherwise stated.

Crystallography. Cell constants at 293 K were determined by a least-squares fit to the setting parameters of 25 independent reflections measured on an Enraf-Nonius CAD4 four-circle diffractometer employing graphite-monochromated Mo-Kα radiation (0.71073 Å) and operating in the ω-2θ scan mode within the range $2 < 2\theta < 50$ Å. Data reduction and empirical absorption corrections (ψ-scans) were performed with the WINGX suite of programs.[72] Structures were solved by direct methods with SHELXS and refined by full-matrix least-squares analysis with SHELXL-97.[73] All non-H

atoms were refined with anisotropic thermal parameters. Aryl and amino H-atoms were included at estimated positions using a riding model. Water and amide H-atoms (if any) were first located from difference maps then restrained at these positions in a manner similar to that employed for the remaining H-atoms. Molecular structure diagrams were produced with ORTEP3.[74] The data in CIF format has been deposited at the Cambridge Crystallographic Data Centre.

Synthesis of Thiobenzhydrazide. Thiobenzhydrazide was prepared using standard procedures.[75−77] Briefly, *S*-(thiobenzoyl)-thioglycolic acid (2.0 g, 9.4 mmol) was dissolved in 1 M NaOH (10 mL, 1 equiv). Water (10 mL) was then added, and this orange solution was cooled in an ice bath. Upon the addition of hydrazine hydrate (1.7 g, 55%, 18.8 mmol), the orange color disappeared. Dilute HCl was added to bring the reaction pH to 5−6 and was allowed to stir for 1 h while cooled in an ice bath. The product was collected by vacuum filtration, washed with chilled water, and air-dried. This crude product was subsequently recrystallized from tepid water to yield thiobenzhydrazide as white crystals, which were stored at 4 °C. Yield 69%. Anal. ($C_7H_8N_2S$) C, H, N. IR (cm^{-1}) 3264m, 3081s, 1589s, 1563s, 1493m, 1449m, 1388w, 1322w, 1309w, 1218m, 1109s, 1074w, 1035w, 1000w, 965m, 904m, 760m, 686s, 638w, 603w. ^{1}H NMR (DMSO-d_6) δ 7.72 (dd, 2H, ArH), 7.49 (m, 3H, ArH). MS (ESI) *m*/*z* 153 (M + H^+).

Pyridoxal Thiobenzoyl Hydrazone (H_2PTBH). Equimolar amounts of pyridoxal hydrochloride (0.47 g, 2.3 mmol) and thiobenzhydrazide (0.35 g, 2.3 mmol) were dissolved in ethanol (100 mL) and refluxed for 30 min with stirring. Upon cooling, the bright orange precipitate was collected by vacuum filtration to yield pure H_2PTBH·0.5H_2O as an orange powder. Yield 70%. Anal. calcd for $C_{15}H_{16}N_3O_{2.5}S$: C, 58.04; H, 5.20; N, 13.54; S, 10.33%. Found: C, 58.14; H, 4.74; N, 12.33; S, 9.60%. IR (cm^{-1}) 3312m, 2692s, 1540m, 1472w, 1453w, 1393w, 1375w, 1320m, 1252s, 1230s, 1155m, 1089m, 1050m, 995m, 960m, 940w, 862w, 813m, 768m, 748m, 689s, 668s, 628w. ^{1}H NMR (DMSO-d_6) δ 13.03 (s, 1H), 9.45 (s, 1H, HC═N), 8.25 (s, 1H, ArH), 8.00 (d, 2H, ArH), 7.65 (d, 1H, ArH), 7.54 (dd, 2H, ArH), 4.81 (s, 2H, CH_2), 2.68 (s, 3H, CH_3). ^{13}C NMR (DMSO-d_6) δ 14.6, 57.9, 127.5, 127.8, 128.2, 129.3, 131.8, 137.2, 138.2, 143.8, 148.6, 152.4, 195.0. MS (ESI) *m*/*z* 302 (M + H^+). All other sulfur analogues were prepared in a similar manner with the appropriate aldehyde or ketone.

Salicylaldehyde Thiobenzoyl Hydrazone (H_2STBH). The H_2STBH monomer was isolated by direct crystallization from the reaction mixture. Yield 88%. Anal. ($C_{14}H_{12}N_2OS$) C, H, N, S. IR (cm^{-1}) 3194m, 3022w, 1606m, 1566w, 1518w, 1480m, 1444m, 1362w, 1331m, 1308w, 1288w, 1264w, 1231w, 1198w, 1152w, 1031w, 952s, 792m, 744s, 683s, 665m, 631m, 577s. ^{1}H NMR (DMSO-d_6) δ 13.61 (s, NH, *Z* isomer), 11.56 (s, OH, *Z* isomer), 10.60 (s, OH, *E* isomer), 9.96 (s, HC═N), 8.89 (s, NH, *E* isomer), 7.86 (d, ArH), 7.34−7.64 (m, ArH), 7.15 (td, ArH), 6.97−7.02 (m, ArH), 6.79−6.87 (m, ArH). MS (ESI) *m*/*z* 257 (M + H^+). The azine disulfide was isolated by further recrystallization of the monomer in hot EtOH.

2-Hydroxy-1-Naphthaldehyde Thiobenzoyl Hydrazone (H_2NTBH). H_2NTBH was collected as small orange crystals, which were suitable for crystallography. Yield 40%. Anal. calcd for $C_{18}H_{14}N_2OS$: C, 70.56; H, 4.61; N, 9.14; S, 10.46%. Found: C, 69.58; H, 4.77; N, 9.22; S, 11.75%. IR (cm^{-1}) 3095w, 2952w, 2870w, 1619m, 1596m, 1564s, 1461m, 1410w, 1340m, 1306w, 1230m, 1182s, 1083m, 974m 939s, 860w, 823s, 774s, 744s, 691s, 664m, 637s. ^{1}H NMR (DMSO-d_6) δ 11.26 (s, 1H), 8.58 (d, 1H, ArH), 8.08−8.14 (m, 2H, ArH), 8.04 (d, 1H, ArH), 7.93 (d, 1H, ArH), 7.54−7.64 (m, 4H, ArH), 7.38−7.45 (m, 2H, ArH). ^{13}C NMR (DMSO-d_6) δ 118.9, 120.3, 123.5, 127.5, 127.8, 127.8, 128.1, 128.9, 131.0, 131.7, 133.7, 139.1, 151.2, 158.4, 191.8. MS (ESI) *m*/*z* 307 (M + H^+).

Di-2-pyridylketone Thiobenzoyl Hydrazone (HPKTBH). HPKTBH was isolated as the cyclic dihydrothiadiazole form. Yield 50%. Anal. ($C_{18}H_{14}N_4S$) C, H, N, S. IR (cm^{-1}) 3253m, 3057w, 1584s, 1567m, 1461m, 1429s, 1295w, 1270m, 1112w, 1100w, 1053m, 979m, 966m, 909m, 756s, 745s, 691s, 673s, 648m, 616m, 577 m. ^{1}H NMR (DMSO-d_6) δ 9.29 (s, 1H, NH), 8.51 (d, 1H, ArH), 7.82−7.89 (m, 4H, ArH), 7.60 (dd, 2H, ArH), 7.41 (m, 3H, ArH), 7.31 (qd, 2H, ArH). ^{13}C NMR (DMSO-d_6) δ 91.2, 120.8, 122.8, 126.0, 128.8, 129.4, 131.1, 137.1, 142.9, 148.6, 161.3. MS (ESI) *m*/*z* 319 (M + H^+).

2-Benzoylpyridine Thiobenzoyl Hydrazone (HBPTBH), HBPTBH was collected as orange needles. Yield 63%. Crystals suitable for X-ray work were obtained from CH_2Cl_2/hexane solution. Anal. ($C_{19}H_{15}N_3S$) C, H, N, S. IR (cm^{-1}) 3040w, 2840w, 1475s, 1459m, 1447m, 1417m, 1315m, 1286w, 1243s, 1152w, 1126s, 1004m, 966s, 797m, 779s, 738s, 702s, 643s, 617 m. ^{1}H NMR (DMSO-d_6) δ 9.32 (s, 1H, NH), 8.57 (d, 1H, ArH), 7.90 (td, 1H, ArH), 7.76 (d, 1H, ArH), 7.59 (d, 2H, ArH) 7.25−7.50 (m, 9H, ArH). ^{13}C NMR (DMSO-d_6) δ 91.1, 120.2, 122.8, 126.0, 126.2, 127.7, 128.2, 128.8, 129.2, 131.3, 137.2, 143.5, 148.9, 161.7. MS (ESI) *m*/*z* 318 (M + H^+).

General Synthesis of the Fe Complexes (Using $Fe^{II}(ClO_4)_2$·6H_2O). The appropriate sulfur ligand (1.1 mmol) was dissolved in 20 mL of acetonitrile, and the nonvolatile base, 1,6-diazabicyclo-[5.4.0]undec-7-ene (0.17 g, 1.1 mmol), was added while purging with nitrogen. $Fe(ClO_4)_2$·6H_2O (0.2 g, 0.55 mmol) was dissolved in 6 mL of nitrogen-purged acetonitrile and was added with stirring to the ligand solution. The mixture was then gently refluxed under nitrogen for 30 min. After cooling, the green product was collected by filtration and washed with acetonitrile.

Fe^{II}(PKTBH)$_2$. Yield 85%. Anal. ($C_{36}H_{26}FeN_8S_2$) C, H, N, S. IR (cm^{-1}) 3051w, 1582m, 1564w, 1510w, 1488w, 1452s, 1414s, 1345s, 1292w, 1279m, 1254w, 1234m, 1201w, 1172w, 1156w, 1116w, 1078m, 1029w, 1016w, 989m, 967m, 944w, 924w, 788m, 764s, 741s, 688s, 662w, 614m, 582s. ^{1}H NMR (DMSO-d_6) δ 8.98 (d, 1H, ArH), 8.59 (d, 1H, ArH), 8.30 (t, 1H, ArH), 8.09 (d, 2H, ArH), 7.87 (d, 1H, ArH) 7.73 (t, 2H, ArH), 7.63 (t, 1H, ArH), 7.48 (t, 1H, ArH), 7.41 (t, 2H, ArH), 7.24 (t, 1H, ArH). Electronic spectrum (MeOH): λ_{max} (nm) (ϵ L mol^{-1} cm^{-1}) 272 (33000), 313 (29500), 372 (22500), 466 (8900), 724 (9500). MS (ESI-positive) *m*/*z* 691 (Fe(PKTBH)$_2$ + H^+). Crystals suitable for X-ray work were obtained by slow evaporation of a 1:1 CH_2Cl_2/MeOH solution.

Fe^{II}(BPTBH)$_2$. Yield 72%. Anal. ($C_{38}H_{28}FeN_6S_2$) C, H, N, S. IR (cm^{-1}) 3055w, 1589w, 1506w, 1445w, 1417s, 1337s, 1300w, 1254w, 1172w, 1069m, 1014m, 999w, 962m, 911w, 781w, 766s, 743s, 721w, 691s, 656 m 625w, 580s. ^{1}H NMR (DMSO-d_6) δ 8.05 (d, 2H, ArH), 8.01 (d, 2H, ArH), 7.88 (d, 1H, ArH), 7.80 (t, 2H, ArH), 7.69 (t, 1H, ArH) 7.61 (t, 1H, ArH), 7.43 (d, 2H, ArH), 7.37 (t, 2H, ArH), 7.23 (t, 1H, ArH). Electronic spectrum (MeOH): λ_{max} (nm) (ϵ L mol^{-1} cm^{-1}) 283 (34100), 368 (20800), 467 (9700), 727 (8100). MS (ESI-positive) *m*/*z* 688 (Fe(BPTBH)$_2$ + H^+).

General Synthesis of the Fe Complexes (Using $Fe^{III}(ClO_4)_3$·6H_2O). The appropriate ligand (0.87 mmol) was dissolved in 20 mL of acetonitrile, and the nonvolatile base, 1,6-diazabicyclo[5.4.0]-undec-7-ene (0.26 g, 1.73 mmol), was added. $Fe(ClO_4)_3$·6H_2O (0.2 g, 0.43 mmol) was dissolved in 6 mL of acetonitrile and added with stirring to the ligand solution. The mixture was then gently refluxed for 30 min. After cooling, the dark product was collected by filtration and washed with acetonitrile.

[Fe^{III}(HPTBH)(PTBH)]·2.75H_2O. The H_2PTBH Fe complex was obtained in the ferric form. Yield 87%. Anal. calcd. for $C_{30}H_{32.5}FeN_6O_{6.75}S_2$: C, 51.10; H, 4.65, N, 11.92; S, 9.09%. Found: C, 51.01; H, 4.13; N, 12.02; S, 8.77%. IR (cm^{-1}) 3462m, 2782m, 2642s, 1621m, 1559w, 1473s, 1421s, 1372s, 1311m, 1221s, 1175w, 1088w, 1037m, 994s, 933s, 827m, 757s, 687s, 645w, 612s, 586w, 556w. Electronic spectrum (MeOH): λ_{max} (nm) (ϵ L mol^{-1} cm^{-1}) 253 (44100), 418 (14400). MS (ESI-positive) *m*/*z* 656 (Fe(HPTBH)-(PTBH) + H^+). Crystals of the complex [Fe(HPTBH)$_2$]Cl·2H_2O were grown from slow evaporation of a 1:1 DMF/MeOH solution of the complex in the presence of a slight excess of NaCl.

$(NMe_4)_2$[Fe^{II}(STBH)$_2$]·0.5NMe_4ClO_4·0.5CH_3CN. NMe_4ClO_4 (75 mg, 0.43 mmol) was added to assist the crystallization of the complex. The H_2STBH Fe complex was obtained in the ferrous form. Yield 67%. Anal. calcd. for $C_{39}H_{51.5}Cl_{0.5}FeN_7O_4S_2$: C, 57.12; H, 6.33, N, 11.96; S, 7.82%. Found: C, 56.72; H, 5.55; N, 11.66; S, 6.57%. IR (cm^{-1}) 3225w, 3110w, 2936w, 1637s, 1579s, 1533m,

1485w, 1465w, 1435s, 1321m, 1287m, 1235w, 1209w, 1193m, 1153w, 1084vs, 966w, 933w, 906w, 850w, 805w, 774m, 755s, 692s, 621s, 569 m. Electronic spectrum (MeOH): λ_{max} (nm) (ϵ L mol^{-1} cm^{-1}) 253 (46900), 397 (14800). MS (ESI-negative) *m*/*z* 564 (Fe(HSTBH)$_2$).

[Fe^{II}(HNTBH)$_2$]·0.5CH$_3$CN. The Fe complex of H_2NTBH was obtained in the ferrous form. Yield 85%. Anal. ($C_{37}H_{27.5}FeN_{4.5}O_2S_2$) C, H, N, S. IR (cm^{-1}) 3136w, 3042w, 1644w, 1613w, 1598m, 1568s, 1530s, 1507w, 1451m, 1423m, 1374s, 1354m, 1332s, 1287m, 1249s, 1189s, 1163w, 1144w, 1094m, 1022m, 968w, 924s, 879w, 827s, 816s, 745s, 673s, 638m, 586m. Electronic spectrum (MeOH): λ_{max} (nm) (ϵ L mol^{-1} cm^{-1}) 267 (52600), 412 (22400), 628 (3600). MS (ESI - negative) *m*/*z* 664 (Fe(HNTBH)$_2$ − H$^+$).

Biological Studies. Cell Culture. The human SK-N-MC neuroepithelioma and MRC-5 fibroblast cell lines were obtained from the American Type Culture Collection (ATCC; Rockville, MD). The cells were grown as described.[9,41,62]

Preparation of ^{59}Fe-Transferrin. Human transferrin (Tf) (Sigma) was labeled with ^{59}Fe (Dupont NEN, MA) to produce $^{59}Fe_2$-Tf (^{59}Fe-Tf), as previously described.[9,78]

Effect of Chelators on Cellular Iron Metabolism. Briefly, SK-N-MC cells were used to study the ability of the chelators to induce ^{59}Fe mobilization from prelabeled cells and prevent ^{59}Fe uptake from ^{59}Fe-Tf.

^{59}Fe Efflux from SK-N-MC Cells. Iron efflux experiments examining the ability of various chelators to mobilize ^{59}Fe from SK-N-MC cells were performed using established techniques.[41,79] Briefly, following prelabeling of cells with ^{59}Fe-Tf (0.75 μM) for 3 h at 37 °C, the cell monolayer was washed four times with ice-cold PBS and then subsequently incubated with each chelator (50 μM). The overlying media containing released ^{59}Fe was then separated from the cells using a pasteur pipet. The cells were removed from the monolayer using a plastic spatula and suspended in PBS (1 mL). Radioactivity was measured in both the cell pellet and supernatant using a γ-scintillation counter (Wallac Wizard 3, Turku, Finland). In these studies, the novel ligands were compared to the previously characterized chelators, DFO, H_2NIH, HDp44mT, and their parent oxygen analogues.[30,32,38,41,71]

Effect of Chelators at Preventing ^{59}Fe Uptake from Tf. The ability of the chelator to prevent cellular ^{59}Fe uptake from the serum Fe transport protein ^{59}Fe-Tf was examined using established techniques.[32,71] Briefly, cells were incubated with ^{59}Fe-Tf (0.75 μM) for 3 h at 37 °C in the presence of each of the chelators (50 μM). The cells were then washed four times with ice-cold PBS and internalized ^{59}Fe was determined by standard techniques by incubating the cell monolayer for 30 min at 4 °C with the general protease, Pronase (1 mg/mL; Sigma).[8,78] The cells were removed from the monolayer using a plastic spatula and centrifuged for 1 min at 14,000 rpm. The supernatant represents membrane-bound Pronase-sensitive ^{59}Fe that is released by the protease, while the internalized ^{59}Fe is the Pronase-insensitive fraction. The novel ligands were compared to the previously characterized chelators, DFO, H_2NIH, HDp44mT, and their parent oxygen analogues.[30,32,38,41,71]

Effect of the Chelators on Cellular Proliferation. This was examined using the MTT (3-(4,5-dimethylthiazol-2-yl)-2,5-diphenyl tetrazolium) assay as described.[41,62] MTT color formation was directly proportional to the number of viable cells measured by Trypan blue staining.[41]

Ascorbate Oxidation Assay. An established protocol was used to measure ascorbate oxidation.[38,63,68,80] Briefly, ascorbic acid (100 μM) was prepared immediately prior to an experiment and incubated in the presence of Fe^{III} (10 μM; added as $FeCl_3$), a 50-fold molar excess of citrate (500 μM), and the chelator (1−60 μM). Absorbance at 265 nm was measured after 10 and 40 min at room temperature and the decrease of intensity between these time points calculated.[68,80]

Benzoate Hydroxylation. This assay employs benzoate as a hydroxyl radical scavenger to generate fluorescent salicylate as a product (308 nm excitation and 410 nm emission) using a well-established protocol.[38,63,68,80] Briefly, benzoic acid (1 mM) was incubated for 1 h at room temperature in 10 mM disodium hydrogen phosphate (pH 7.4) with 5 mM hydrogen peroxide, the Fe chelator (3−180 μM) and ferrous sulfate (30 μM). All solutions were prepared immediately prior to use and the Fe^{II} added to water that had been extensively purged with nitrogen. The addition of Fe was used to start the reaction, and the solution was kept in the dark prior to measuring the fluorescence using a Perkin-Elmer L550B spectrofluorometer. In these experiments, salicylate was used as a standard and to determine quenching by the chelators.[68,80]

Statistical Analysis. Experimental data were compared using Student's *t*-test. Results were expressed as the mean or mean ± SD (number of experiments) and considered to be statistically significant when $p < 0.05$.

Acknowledgment. D.R.R. and P.V.B. thank the Australian Research Council (DP0450001 and DP0773027) for research grant funding. D.R.R. acknowledges the National Health and Medical Research Council of Australia for grant and fellowship support. D.K. is the grateful recipient of an Australian Postgraduate Award from the University of Sydney.

Supporting Information Available: Elemental analysis data. This material is available free of charge via the Internet at http://pubs.acs.org.

References

(1) Bergeron, R. J.; Bharti, N.; Wiegand, J.; McManis, J. S.; Yao, H.; et al. Polyamine-vectored iron chelators: the role of charge. *J. Med. Chem.* **2005**, *48*, 4120−4137.
(2) Bergeron, R. J.; Wiegand, J.; McManis, J. S.; Bharti, N. The design, synthesis, and evaluation of organ-specific iron chelators. *J. Med. Chem.* **2006**, *49*, 7032−7043.
(3) Bergeron, R. J.; Wiegand, J.; Bharti, N.; Singh, S.; Rocca, J. R. Impact of the 3,6,9-trioxadecyloxy group on desazadesferrithiocin analogue iron clearance and organ distribution. *J. Med. Chem.* **2007**, *50*, 3302−3313.
(4) Buss, J. L.; Greene, B. T.; Turner, J.; Torti, F. M.; Torti, S. V. Iron chelators in cancer chemotherapy. *Curr. Top. Med. Chem.* **2004**, *4*, 1623−1635.
(5) Kalinowski, D. S.; Richardson, D. R. The evolution of iron chelators for the treatment of iron overload disease and cancer. *Pharmacol. Rev.* **2005**, *57*, 547−583.
(6) Liu, Z. D.; Hider, R. C. Design of iron chelators with therapeutic application. *Coord. Chem. Rev.* **2002**, *232*, 151−171.
(7) Trinder, D.; Zak, O.; Aisen, P. Transferrin receptor-independent uptake of differic transferrin by human hepatoma cells with antisense inhibition of receptor expression. *Hepatology* **1996**, *23*, 1512−1520.
(8) Richardson, D. R.; Baker, E. The uptake of iron and transferrin by the human malignant melanoma cell. *Biochim. Biophys. Acta* **1990**, *1053*, 1−12.
(9) Richardson, D.; Baker, E. Two mechanisms of iron uptake from transferrin by melanoma cells. The effect of desferrioxamine and ferric ammonium citrate. *J. Biol. Chem.* **1992**, *267*, 13972−13979.
(10) Thelander, L.; Reichard, P. Reduction of ribonucleotides. *Annu. Rev. Biochem.* **1979**, *48*, 133−158.
(11) Thelander, L.; Graslund, A.; Thelander, M. Continual presence of oxygen and iron is required for mammalian ribonucleotide reduction: possible regulation mechanism. *Biochem. Biophys. Res. Commun.* **1983**, *110*, 859−865.
(12) Elford, H. L.; Freese, M.; Passamani, E.; Morris, H. P. Ribonucleotide reductase and cell proliferation. I. Variations of ribonucleotide reductase activity with tumor growth rate in a series of rat hepatomas. *J. Biol. Chem.* **1970**, *245*, 5228−5233.
(13) Kolberg, M.; Strand, K. R.; Graff, P.; Andersson, K. K. Structure, function, and mechanism of ribonucleotide reductases. *Biochim. Biophys. Acta* **2004**, *1699*, 1−34.
(14) Gao, J.; Richardson, D. R. The potential of iron chelators of the pyridoxal isonicotinoyl hydrazone class as effective anti-proliferative agents IV. The mechanisms involved in inhibiting cell cycle progression. *Blood* **2001**, *98*, 842−850.
(15) Liang, S.; Richardson, D. R. The effect of potent iron chelators on the regulation of p53: examination of the expression, localization and DNA-binding activity of p53 and the transactivation of WAF1. *Carcinogenesis* **2003**, *24*, 1601−1614.
(16) Fu, D.; Richardson, D. R. Iron chelation and regulation of the cell-cycle: two mechanisms of post-transcriptional regulation of the universal cyclin-dependent kinase inhibitor p21CIP1/WAF1 by iron depletion. *Blood* **2007**, *110*, 752−761.

(17) Nurtjahja-Tjendraputra, E.; Fu, D.; Phang, J. M.; Richardson, D. R. Iron chelation regulates cyclin D1 expression via the proteasome: a link to iron deficiency-mediated growth suppression. *Blood* **2007**, *109*, 4045−4054.
(18) Le, N. T.; Richardson, D. R. Iron chelators with high antiproliferative activity up-regulate the expression of a growth inhibitory and metastasis suppressor gene: a link between iron metabolism and proliferation. *Blood* **2004**, *104*, 2967−2975.
(19) Yu, Y.; Kovacevic, Z.; Richardson, D. R. Tuning cell cycle regulation with an iron key. *Cell Cycle* **2007**, *6*, 1982−1994.
(20) Zhao, R.; Planalp, R. P.; Ma, R.; Greene, B. T.; Jones, B. T.; et al. Role of zinc and iron chelation in apoptosis mediated by tachpyridine, an anti-cancer iron chelator. *Biochem. Pharmacol.* **2004**, *67*, 1677−1688.
(21) Torti, S. V.; Torti, F. M.; Whitman, S. P.; Brechbiel, M. W.; Park, G.; et al. Tumor cell cytotoxicity of a novel metal chelator. *Blood* **1998**, *92*, 1384−1389.
(22) Gojo, I.; Tidwell, M. L.; Greer, J.; Takebe, N.; Seiter, K.; et al. Phase I and pharmacokinetic study of Triapine((R)), a potent ribonucleotide reductase inhibitor, in adults with advanced hematologic malignancies. *Leuk. Res.* **2007**, *31*, 1173−1181.
(23) Finch, R. A.; Liu, M. C.; Cory, A. H.; Cory, J. G.; Sartorelli, A. C. Triapine (3-aminopyridine-2-carboxaldehyde thiosemicarbazone; 3-AP): an inhibitor of ribonucleotide reductase with antineoplastic activity. *Adv. Enzyme Regul.* **1999**, *39*, 3−12.
(24) Feun, L.; Modiano, M.; Lee, K.; Mao, J.; Marini, A. et al. Phase I and pharmacokinetic study of 3-aminopyridine-2-carboxaldehyde thiosemicarbazone (3-AP) using a single intravenous dose schedule. *Cancer Chemother. Pharmacol.* **2002**, *50*, 223−229.
(25) Rakba, N.; Loyer, P.; Gilot, D.; Delcros, J. G.; Glaise, D. et al. Antiproliferative and apoptotic effects of O-Trensox, a new synthetic iron chelator, on differentiated human hepatoma cell lines. *Carcinogenesis* **2000**, *21*, 943−951.
(26) Ponka, P.; Borova, J.; Neuwirt, J.; Fuchs, O. Mobilization of iron from reticulocytes. Identification of pyridoxal isonicotinoyl hydrazone as a new iron chelating agent. *FEBS Lett.* **1979**, *97*, 317−321.
(27) Ponka, P.; Borova, J.; Neuwirt, J.; Fuchs, O.; Necas, E. A study of intracellular iron metabolism using pyridoxal isonicotinoyl hydrazone and other synthetic chelating agents. *Biochim. Biophys. Acta* **1979**, *586*, 278−297.
(28) Ponka, P.; Richardson, D.; Baker, E.; Schulman, H. M.; Edward, J. T. Effect of pyridoxal isonicotinoyl hydrazone (PIH) and other hydrazones on iron release from macrophages, reticulocytes and hepatocytes. *Biochim. Biophys. Acta* **1988**, *967*, 122−129.
(29) Lovejoy, D. B.; Richardson, D. R. Novel "hybrid" iron chelators derived from aroylhydrazones and thiosemicarbazones demonstrate selective antiproliferative activity against tumor cells. *Blood* **2002**, *100*, 666−676.
(30) Becker, E. M.; Lovejoy, D. B.; Greer, J. M.; Watts, R.; Richardson, D. R. Identification of the di-pyridyl ketone isonicotinoyl hydrazone (PKIH) analogues as potent iron chelators and anti-tumour agents. *Br. J. Pharmacol.* **2003**, *138*, 819−830.
(31) Yu, Y.; Wong, J.; Lovejoy, D. B.; Kalinowski, D. S.; Richardson, D. R. Chelators at the cancer coalface: desferrioxamine to Triapine and beyond. *Clin. Cancer Res.* **2006**, *12*, 6876−6883.
(32) Yuan, J.; Lovejoy, D. B.; Richardson, D. R. Novel di-2-pyridyl-derived iron chelators with marked and selective antitumor activity: in vitro and in vivo assessment. *Blood* **2004**, *104*, 1450−1458.
(33) Richardson, D. R.; Sharpe, P. C.; Lovejoy, D. B.; Senaratne, D.; Kalinowski, D. S.; et al. Dipyridyl thiosemicarbazone chelators with potent and selective antitumor activity form iron complexes with redox activity. *J. Med. Chem.* **2006**, *49*, 6510−6521.
(34) Kalinowski, D. S.; Richardson, D. R. Future of toxicology-iron chelators and differing modes of action and toxicity: the changing face of iron chelation therapy. *Chem. Res. Toxicol.* **2007**, *20*, 715−720.
(35) Kalinowski, D. S.; Yu, Y.; Sharpe, P. S.; Islam, M.; Liao, Y.-T.; et al. Design, synthesis and characterization of novel iron chelators: Structure-activity relationships of the 2-benzoylpyridine thiosemicarbazone series and their 3-nitrobenzoyl analogs as potent anti-tumor agents. *J. Med. Chem.* **2007**, *50*, 3716−3729.
(36) Buss, J. L.; Neuzil, J.; Ponka, P. Oxidative stress mediates toxicity of pyridoxal isonicotinoyl hydrazone analogs. *Arch. Biochem. Biophys.* **2004**, *421*, 1−9.
(37) Barnham, K. J.; Masters, C. L.; Bush, A. I. Neurodegenerative diseases and oxidative stress. *Nat. Rev. Drug Discovery* **2004**, *3*, 205−214.
(38) Bernhardt, P. V.; Caldwell, L. M.; Chaston, T. B.; Chin, P.; Richardson, D. R. Cytotoxic iron chelators: characterization of the structure, solution chemistry and redox activity of ligands and iron complexes of the di-2-pyridyl ketone isonicotinoyl hydrazone (HPKIH) analogues. *J. Biol. Inorg. Chem.* **2003**, *8*, 866−880.
(39) Chaston, T. B.; Watts, R. N.; Yuan, J.; Richardson, D. R. Potent antitumor activity of novel iron chelators derived from di-2-pyridylketone isonicotinoyl hydrazone involves fenton-derived free radical generation. *Clin. Cancer Res.* **2004**, *10*, 7365−7374.
(40) Whitnall, M.; Howard, J.; Ponka, P.; Richardson, D. R. A class of iron chelators with a wide spectrum of potent antitumor activity that overcomes resistance to chemotherapeutics. *Proc. Natl. Acad. Sci. U.S.A.* **2006**, *103*, 14901−14906.
(41) Richardson, D. R.; Tran, E. H.; Ponka, P. The potential of iron chelators of the pyridoxal isonicotinoyl hydrazone class as effective antiproliferative agents. *Blood* **1995**, *86*, 4295−4306.
(42) Baker, E.; Richardson, D. R.; Gross, S.; Ponka, P. Evaluation of the iron chelation potential of hydrazones of pyridoxal, salicylaldehyde and 2-hydroxy-1-naphthylaldehyde using the hepatocyte in culture. *Hepatology* **1992**, *15*, 492−501.
(43) Zelenin, K. N.; Alekseev, V. A.; Khrustalev, V. A.; Yakimovich, S. I.; Nikolaev, V. N.; et al. Ring-ring and ring-chain tautomerism of thiobenzoylhydrazones of aliphatic beta-dicarbonyl compounds. *Zh. Org. Khim.* **1984**, *20*, 180−187.
(44) Jensen, K. A.; Pedersen, C. Studies of thio acids and their derivatives. IV. 1,2,3,4-Thiatriazoles. *Acta Chem. Scand.* **1961**, *15*, 1104−1108.
(45) Jensen, K. A.; Pedersen, C. Studies of thio acids and their derivatives. III. Methods for the preparation of thiohydrazides. *Acta Chem. Scand.* **1961**, *15*, 1097−1103.
(46) Pelagatti, P.; Venturini, A.; Leporati, A.; Carcelli, M.; Costa, M.; et al. Chemoselective homogeneous hydrogenation of phenylacetylene using thiosemicarbazone and thiobenzoylhydrazone palladium(II) complexes as catalysts. *J. Chem. Soc., Dalton Trans.* **1998**, *16*, 2715−2722.
(47) Singh, N. K.; Singh, D. K.; Singh, J. Synthesis, characterization and biological activity of the complexes of manganese(III), cobalt(III), nickel(II), copper(II) and zinc(II) with salicylaldehyde thiobenzhydrazone. *Indian J. Chem., Sect. A* **2001**, *40A*, 1064−1069.
(48) Stoyanov, S.; Antonov, L.; Karagiannidis, P.; Akrivos, P. Thione-disulfide interchange of some heterocyclic tautomeric thiones and their symmetrical disulfides. *Monatsh. Chem.* **1996**, *127*, 495−504.
(49) Stoyanov, S.; Petkov, I.; Antonov, L.; Stoyanova, T.; Karagiannidis, P.; et al. Thione-thiol tautomerism and stability of 2- and 4-mercaptopyridines and 2-mercaptopyrimidines. *Can. J. Chem.* **1990**, *68*, 1482−1489.
(50) Stoyanov, S.; Stoyanova, T.; Akrivos, P. Spectral and theoretical stidies on thione-thiol tautomerism of N-containing heterocycles. *Trends Appl. Spectrosc.* **1998**, *2*, 89−103.
(51) Stoyanov, S.; Stoyanova, T.; Akrivos, P.; Karagiannidis, P.; Nikolov, P. Spectroscopic and computational investigation of the ground and low excited states of some symmetrical heterocyclic disulfides. *J. Heterocycl. Chem.* **1996**, *33*, 927−931.
(52) Richardson, D. R.; Bernhardt, P. Crystal and molecular structure of 2-hydroxy-1-naphthylaldehyde isonicotinoyl hydrazone (NIH) and its iron(III) complex: An iron chelator with anti-proliferative activity. *J. Biol. Inorg. Chem.* **1999**, *4*, 266−273.
(53) Zelenin, K. N.; Alekseev, V. V.; Khrustalev, V. A. Synthesis and structure of (thioacyl)hydrazones. *Zh. Org. Khim.* **1984**, *20*, 169−180.
(54) Evans, M.; Hill, L.; Taylor, D. R.; Myers, M. Thiadiazoles and dihydrothiadiazoles. Part 5. Synthesis of 2,3-dihydro-1,3,4-thiadiazoles by reaction of aldehydes or ketones with thioaroylhydrazines. *J. Chem. Soc., Perkin Trans. I* **1986**, *8*, 1499−1505.
(55) Alekseev, V. V.; Khrustalev, V. A.; Zelenin, K. N. Tautomerism of thioacylhydrazone and 1,3,4-thiadiazol-2-ine. *Khim. Geterotsikl. Soedin.* **1981**, *11*, 1569−1570.
(56) Zelenin, K. N.; Khorseeva, L. A.; Alekseev, V. V.; Arapov, O. V. Thiobenzoylhydrazone complexes. *Zh. Obshch. Khim.* **1988**, *58*, 237−238.
(57) Yusupov, V. G.; Toshev, M. T.; Saidov, S. O.; Dustov, K. B.; Zelenin, K. N.; et al. Crystal and molecular structure of condensation products of acetone with thiobenzoylhydrazine and its copper(II) and nickel(II) complexes. *Zh. Neorg. Khim.* **1992**, *37*, 1039−1046.
(58) Richardson, D. R.; Wis Vitolo, L. M.; Hefter, G. T.; May, P. M.; Clare, B. W.; Webb, J.; Wilairat, P. Iron chelators of the pyridoxal isonicotinoyl hydrazone class Part I. Ionization characteristics of the ligands and their relevance to biological properties. *Inorg. Chim. Acta* **1990**, *170*, 165−170.
(59) Armstrong, C. M.; Bernhardt, P. V.; Chin, P.; Richardson, D. R. Structural variations and formation constants of first-row transition metal complexes of biologically active aroylhydrazones. *Eur. J. Inorg. Chem.* **2003**, 1145−1156.
(60) Bernhardt, P. V.; Mattsson, J.; Richardson, D. R. Complexes of cytotoxic chelators from the dipyridyl ketone isonicotinoyl hydrazone (HPKIH) analogues. *Inorg. Chem.* **2006**, *45*, 752−760.

(61) Darnell, G.; Richardson, D. R. The potential of iron chelators of the pyridoxal isonicotinoyl hydrazone class as effective antiproliferative agents III: the effect of the ligands on molecular targets involved in proliferation. *Blood* **1999**, *94*, 781−792.
(62) Richardson, D. R.; Milnes, K. The potential of iron chelators of the pyridoxal isonicotinoyl hydrazone class as effective antiproliferative agents II: the mechanism of action of ligands derived from salicylaldehyde benzoyl hydrazone and 2-hydroxy-1-naphthylaldehyde benzoyl hydrazone. *Blood* **1997**, *89*, 3025−3038.
(63) Chaston, T. B.; Lovejoy, D. B.; Watts, R. N.; Richardson, D. R. Examination of the antiproliferative activity of iron chelators: multiple cellular targets and the different mechanism of action of triapine compared with desferrioxamine and the potent pyridoxal isonicotinoyl hydrazone analogue 311. *Clin. Cancer Res.* **2003**, *9*, 402−414.
(64) Johnson, D. K.; Pippard, M. J.; Murphy, T. B.; Rose, N. J. An in vivo evaluation of iron-chelating drugs derived from pyridoxal and its analogs. *J. Pharmacol. Exp. Ther.* **1982**, *221*, 399−403.
(65) Richardson, D. R. Cytotoxic analogs of the iron(III) chelator pyridoxal isonicotinoyl hydrazone: effects of complexation with copper(II), gallium(III), and iron (III) on their antiproliferative activities. *Antimicrob. Agents Chemother.* **1997**, *41*, 2061−2063.
(66) Richardson, D. R.; Ponka, P. The iron metabolism of the human neuroblastoma cell: lack of relationship between the efficacy of iron chelation and the inhibition of DNA synthesis. *J. Lab. Clin. Med.* **1994**, *124*, 660−671.
(67) Chaston, T. B.; Richardson, D. R. Iron chelators for the treatment of iron overload disease: relationship between structure, redox activity, and toxicity. *Am. J. Hematol.* **2003**, *73*, 200−210.
(68) Chaston, T. B.; Richardson, D. R. Interactions of the pyridine-2-carboxaldehyde isonicotinoyl hydrazone class of chelators with iron and DNA: implications for toxicity in the treatment of iron overload disease. *J. Biol. Inorg. Chem.* **2003**, *8*, 427−438.
(69) Bernhardt, P. V.; Wilson, G. J.; Sharpe, P. C.; Kalinowski, D. S.; Richardson, D. R. Tuning the anti-proliferative activity of biologically active iron chelators: characterisation of the coordination chemistry and biological efficacy of 2-acetylpyridine and 2-benzoylpyridine hydrazone ligands. *J. Biol. Inorg. Chem.* **2007**, in press.
(70) Edward, J. T.; Gauthier, M.; Chubb, F. L.; Ponka, P. Synthesis of new acylhydrazones as iron-chelating compounds. *J. Chem. Eng. Data* **1988**, *33*, 538−540.
(71) Becker, E.; Richardson, D. R. Development of novel aroylhydrazone ligands for iron chelation therapy: 2-pyridylcarboxaldehyde isonicotinoyl hydrazone analogs. *J. Lab. Clin. Med.* **1999**, *134*, 510−521.
(72) Farrugia, L. J. WINGX - An integrated system of windows programs for the solution, refinement and analysis of single crystal X-ray diffraction data. *J. Appl. Crystallogr.* **1999**, *32*, 837−838.
(73) Sheldrick, G. M. *SHELX97. Programs for Crystal Structure Analysis*, Release 97-92; University of Göttingen: Göttingen, Germany.
(74) Farrugia, L. J. ORTEP-3 for windows - a version of ORTEP-III with a graphical user interface (GUI). *J. Appl. Crystallogr.* **1997**, *30*, 565.
(75) Holmberg, B. Benzoyl- and thiobenzoylthioglycolic acids and thiobenzohydrazide. *Arkiv. Kemi. Mineral Geol.* **1944**, *17A*, 23.
(76) Singh, N. K.; Singh, S. B. Antitumour and immunomodulatory effects of Cu(II) complexes of thiobenzoylhydrazide. *Met.-Based Drugs* **2002**, *9*, 109−118.
(77) Shome, S. C.; Gangopadhyay, P. K.; Gangopadhyay, S. Extraction and spectrophotometric determination of ruthenium and osmium with thiobenzhydrazide. *Talanta* **1976**, *23*, 603−605.
(78) Richardson, D. R.; Baker, E. Intermediate steps in cellular iron uptake from transferrin. Detection of a cytoplasmic pool of iron, free of transferrin. *J. Biol. Chem.* **1992**, *267*, 21384−21389.
(79) Richardson, D. R. Mobilization of iron from neoplastic cells by some iron chelators is an energy-dependent process. *Biochim. Biophys. Acta* **1997**, *1320*, 45−57.
(80) Dean, R. T.; Nicholson, P. The action of nine chelators on iron-dependent radical damage. *Free Radical Res.* **1994**, *20*, 83−101.

JM070839Q